Contrib Mineral Petrol (2010) 160:467–487
DOI 10.1007/s00410-010-0489-z

ORIGINAL PAPER

Relative contributions of crust and mantle to generation of Campanian high-K calc-alkaline I-type granitoids in a subduction setting, with special reference to the Harşit Pluton, Eastern Turkey

Orhan Karsli · Abdurrahman Dokuz · İbrahim Uysal · Faruk Aydin · Bin Chen · Raif Kandemir · Jan Wijbrans

Received: 15 May 2009 / Accepted: 11 January 2010 / Published online: 2 February 2010

Abstract We present elemental and Sr–Nd–Pb isotopic data for the magmatic suite (~79 Ma) of the Harşit pluton, from the Eastern Pontides (NE Turkey), with the aim of determining its magma source and geodynamic evolution. The pluton comprises granite, granodiorite, tonalite and minor diorite (SiO_2 = 59.43–76.95 wt%), with only minor gabbroic diorite mafic microgranular enclaves in composition (SiO_2 = 54.95–56.32 wt%), and exhibits low Mg# (<46). All samples show a high-K calc-alkaline differentiation trend and I-type features. The chondrite-normalized REE patterns are fractionated [$(La/Yb)_n$ = 2.40–12.44] and display weak Eu anomalies (Eu/Eu* = 0.30–0.76). The rocks are characterized by enrichment of LILE and depletion of HFSE. The Harşit host rocks have weak concave-upward REE patterns, suggesting that amphibole and garnet played a significant role in their generation during magma segregation. The host rocks and their enclaves are isotopically indistinguishable. Sr–Nd isotopic data for all of the samples display I_{Sr} = 0.70676–0.70708, ε_{Nd}(79 Ma) = −4.4 to −3.3, with T_{DM} = 1.09–1.36 Ga. The lead isotopic ratios are ($^{206}Pb/^{204}Pb$) = 18.79–18.87, ($^{207}Pb/^{204}Pb$) = 15.59–15.61 and ($^{208}Pb/^{204}Pb$) = 38.71–38.83. These geochemical data rule out pure crustal-derived magma genesis in a post-collision extensional stage and suggest mixed-origin magma generation in a subduction setting. The melting that generated these high-K granitoidic rocks may have resulted from the upper Cretaceous subduction of the Izmir–Ankara–Erzincan oceanic slab beneath the Eurasian block in the region. The back-arc extensional events would have caused melting of the enriched subcontinental lithospheric mantle and formed mafic magma. The underplating of the lower crust by mafic magmas would have played a significant role in the generation of high-K magma. Thus, a thermal anomaly induced by underplated basic magma into a hot crust would have caused partial melting in the lower part of the crust. In this scenario, the lithospheric mantle-derived basaltic melt first mixed with granitic magma of crustal origin at depth. Then, the melts, which subsequently underwent a fractional crystallization and crustal assimilation processes, could ascend to shallower crustal levels to generate a variety of rock types ranging from diorite to granite. Sr–Nd isotope modeling shows that the generation of these magmas involved ~65–75% of the lower crustal-derived melt and ~25–35% of subcontinental lithospheric mantle. Further, geochemical data and the Ar–Ar plateau age on hornblende, combined with regional studies, imply that the

Communicated by G. Moore.

Electronic supplementary material The online version of this article (doi:10.1007/s00410-010-0489-z) contains supplementary material, which is available to authorized users.

O. Karsli (✉) · A. Dokuz · R. Kandemir
Department of Geological Engineering, Gümüşhane University, 29000 Gümüşhane, Turkey
e-mail: okarsli@gmail.com

İ. Uysal
Department of Geological Engineering, Karadeniz Technical University, 61100 Trabzon, Turkey

F. Aydin
Department of Geological Engineering, Niğde University, 51200 Niğde, Turkey

B. Chen
School of Earth and Space Sciences, Peking University, Beijing 100871, China

J. Wijbrans
Laboratory of Isotope Geology, Vrije University, De Boelelaan 1085, 1081 HV Amsterdam, The Netherlands

Harşit pluton formed in a subduction setting and that the back-arc extensional period started by least ~79 Ma in the Eastern Pontides.

Keywords Eastern Turkey · High-K calc-alkaline granitoids · Lower crustal melting · Subduction setting · Back-arc extension · Radiogenic isotopes

Introduction

Granitoids are the major component of the continental crust on Earth. Hence, the growth of the continent hinges largely on the mode of generation of granitoid rocks. As main components of the continental crust, granitoids also give pivotal clues to lithospheric evolution and tectonics. They are genetically classified as being of either mantle origin (e.g., Turner et al. 1992; Han et al. 1997; Volkert et al. 2000), mixed origin, with various proportions of crust- and mantle-derived components (e.g., Poli and Tommasini 1991; Barbarin and Didier 1992; Wiebe 1996; Altherr et al. 2000; Chen et al. 2002; Bonin 2004; Karsli et al. 2007) or crustal origin (e.g., Chappell and White 1992; Chappell 1999). The high-K calc-alkaline granitoids in a subduction zone are distinct from the other types based on their major, trace element and isotope compositions but are widely distributed in space and time. Their petrogenesis and geodynamic settings are still a subject of considerable controversy. Some petrogenetic models have been proposed for the origin of high-K calc-alkaline I-type granitoids, including fractionation of hybrid magma forming various contributions of crustal and mantle end-members in both subduction zone and post-collision extensional settings. Following their origins constitute one of the most important processes with regard to evolution of the continental crust. Although this type of granitoid can occur in extensional settings with the partial melting of the lower crust by underplated basaltic magma (Sonder et al. 1987; Windley 1991; Frost et al. 1998; Chen and Jahn 2004), high-K calc-alkaline rock is likely to have formed by partial fusion of the mafic lower crust, with extra heating by underplated basaltic magma in even a collision setting (e.g., Roberts and Clemens 1993; Flierdt et al. 2003). Therefore, these types of rocks are commonly interpreted as magmatic precursors to crustal and mantle melting processes and are regarded as a potentially important tracer in understanding the petrogenesis and geodynamics of granitoid rocks of mixed origin.

Several plutons were studied to identify their genesis and the geodynamics of the eastern Pontides (e.g., Yilmaz and Boztuğ 1996; Karsli et al. 2004a, b; Boztuğ et al. 2004, 2006; Topuz et al. 2005; Dokuz et al. 2006, 2010; Karsli et al. 2007; Kaygusuz et al. 2008; Dokuz 2009), but little effort has been made to combine the tectonic and petrological data in order to contribute to the understanding of the geodynamic evolution of the Eastern Pontides. The isotopic and geochronological data in the region are very limited. However, we think that the eastern Pontide region may be an ideal place to test the underplating theory and to interpret how the high-K calc-alkaline granitoids were generated in a subduction setting. The granitoids studied here exhibit compositional ranges from gabbroic diorite to granite, and confirming the crustal and mantle source components for the rocks will permit development of better-constrained geodynamic models. Accordingly, this contribution reports petrographic, whole-rock geochemical, Sr–Nd–Pb isotopic and Ar–Ar age characteristics of the Harşit pluton in the Eastern Pontides, NE Turkey. These data are then used to shed light on the nature of the particular type of magmatism and tectonic setting of the pluton, particularly in relation to the initiation of back-arc extensional events and the duration of Neotethys subduction.

Geological setting

Anatolia is ascribed as a geologically complex domain in the Alpine–Himalayan fold-thrust fault belt. It is a continental block migrating westwards in response to the continuing north–south convergence between Eurasia and Africa–Arabia during the late Cenozoic. This convergence is accommodated by two major strike–slip faults, the North Anatolian Fault (NAF) and the East Anatolian Fault (EAF) (e.g. Şengör and Yilmaz 1981; Koçyiğit et al. 2001) (Fig. 1a). Turkey is formed by mainly four major tectonic blocks, separated by three main high-pressure (HP) belts (e.g., Okay and Tüysüz 1999). These are the Intra-Pontide suture, separating the Istanbul zone from the Sakarya Block to the NW, the Izmir–Ankara suture prolonged to the East by the Izmir–Ankara–Erzincan suture separating the Sakarya Block from the Anatolide–Taurides Block in the center, and the Assyrian–Zagros suture separating the Anatolide–Taurides from the Arabian plate to the SE and the Pamphylian Suture in SSW Turkey (Fig. 1a).

The Eastern Pontides which are subset of Sakarya Series is an ensialic, south-facing magmatic arc of Albian to Oligocene age. It formed by north-dipping subduction under the Eurasian continental margin (e.g., Akin 1979; Şengör and Yilmaz 1981; Okay and Şahintürk 1997; Yilmaz et al. 1997; Şengör et al. 2003) and the subsequent collision between the Pontides and the Tauride–Anatolide platforms, although the timing of the collision is still controversial (e.g., Robinson et al. 1995; Okay and Şahintürk 1997; Şen et al. 1998; Şengör et al. 2003). Okay et al. (1997) suggested that the collision should date back

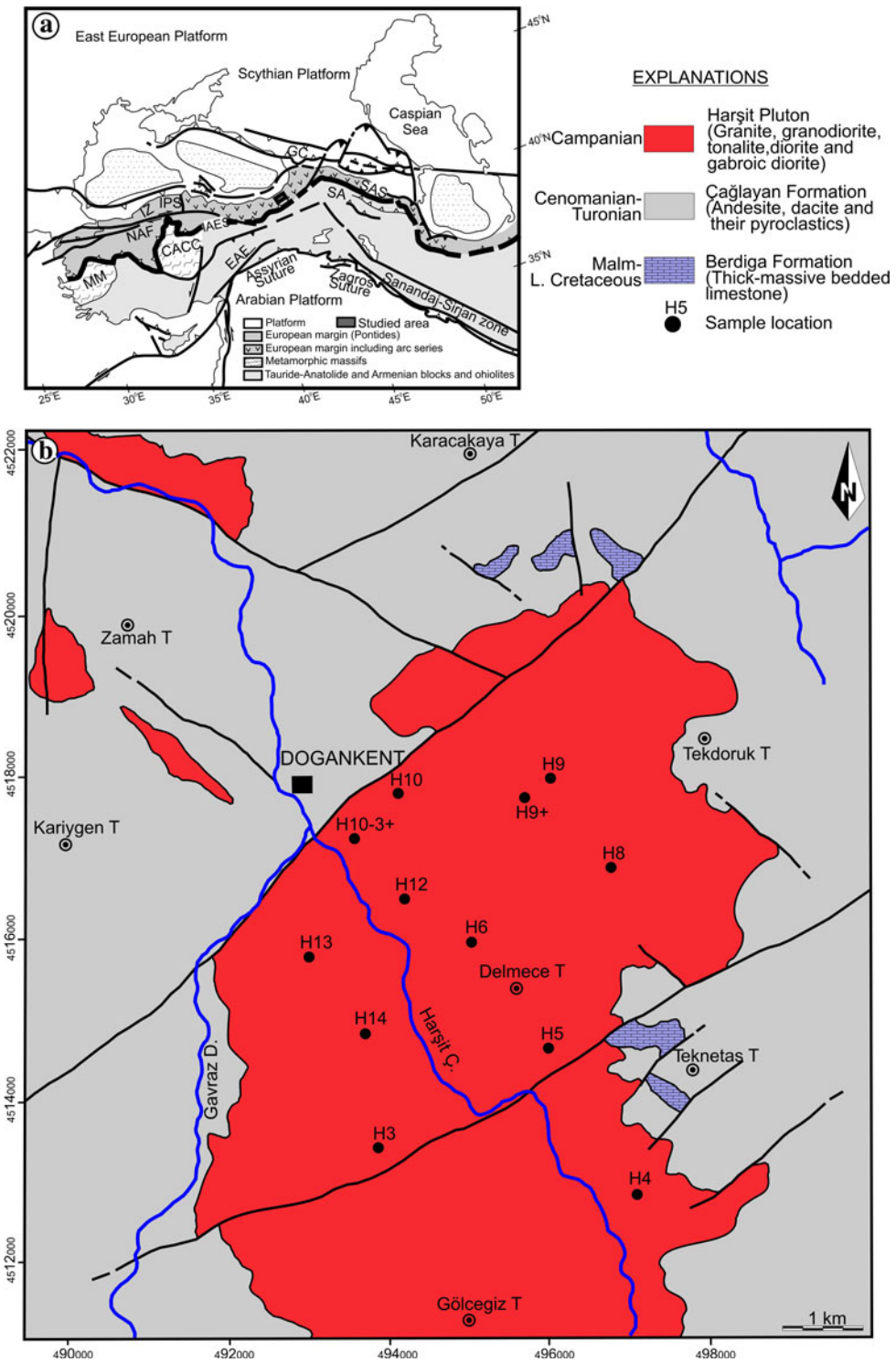

Fig. 1 **a** Global tectonic map of Turkey, with main blocks and suture zones [modified from Avagyan et al. (2005)]. *IAES* Izmir–Ankara–Erzincan suture, *IPS* Intra-Pontide suture, *IZ* Istanbul Zone, *MM* Menderes massif, *NAF* North Anatolian Fault, *EAF* East Anatolian Fault, *GC* Great Caucasus, *CACC* Central Anatolian Crystalline Complex, *SA* South Armenian block, *SAS* Sevan–Akera suture. **b** Simplified geological map of the Harşit area showing the Campanian granitoid rocks

to late Paleocene to early Eocene, based on field relationships and ages of granitoids. The basement of Eastern Pontides consists of Devonian metamorphic rocks, Lower Carboniferous granitic and dacitic rocks, Upper Carboniferous–Lower Permian shallow-marine to terrigenous sedimentary rocks and Permo-Triassic metabasalt–phyllite–marble (e.g., Yilmaz 1972; Şengör and Yilmaz 1981; Okay and Şahintürk 1997; Yilmaz et al. 1997). The basement is overlain by Lower and Middle Jurassic tuffs, pyroclastic and interbedded clastic sedimentary rocks, and Upper Jurassic–Lower Cretaceous carbonates (Şengör and Yilmaz 1981; Okay and Şahintürk 1997). An extensive zone of backthrusting brought ophiolitic mélange nappes of Cretaceous age into its southern margin (e.g., Yilmaz et al.

1997; Şengör et al. 2003). These are the hintermost parts of the Eastern Anatolian Accretionary Complex. Late Mesozoic and early Cenozoic times are recorded by volcanic and granitoidic rocks (e.g., Tokel 1977; Yilmaz and Boztuğ 1996; Boztuğ et al. 2004; Karsli et al. 2007; Kaygusuz et al. 2008) The granitoid bodies occurred in various geodynamic settings and have different ages (e.g., Moore et al. 1980) and compositions (Yilmaz and Boztuğ 1996; Karsli et al. 2002; Topuz et al. 2005; Boztuğ et al. 2006; Dokuz et al. 2006). The emplacements took place during the processes of crustal thickening related to the arc–continent collision and subsequent post-collisional extensional regimes (e.g., Yilmaz and Boztuğ 1996; Karsli et al. 2004a, b; Topuz et al. 2005). These units are covered by Upper Paleocene–Lower Eocene major foreland flysch and Post-Eocene terrigenous units (e.g., Okay and Şahintürk 1997).

The Harşit pluton form outcrops with length less than 20 km and width maximum 10 km. The pluton is a part of the composite Kaçkar Batholith, dated 30–80 Ma (K–Ar on hornblende; Taner 1977; Moore et al. 1980). The Kaçkar batholith lies along an E–W trend in the eastern Pontides of Eastern Turkey. The Harşit pluton is located in the northern part of the eastern Pontides and has a wide contact aureole in Cenomanian–Turonian andesitic rocks of the Çağlayan Formation (Fig. 1b). It is made of a variety of rock types including granite, granodiorite, tonalite and diorite, with tonalite dominance ($\sim$80% of the mass volume). All the rock units share several common petrographic features and hence are described together. Diorite never exceed 15 volume%. Granite occupies less than 5% of the volume. The contact relations between all lithotypes are transitional. The plutons were dated at $\sim$79 Ma using Ar–Ar method on hornblende separate in this study.

Analytical techniques

Twelve samples were taken from the Harşit pluton. Major, trace and rare earth element contents were determined at the commercial ACME Laboratories Ltd in Vancouver, Canada. Major elements were measured by ICP-AES after fusion with $LiBO_2$. Major element detection limits are about 0.001–0.04%. For the trace and rare earth elements, 0.2 g sample powder and 1.5 g $LiBO_2$ flux were mixed in a graphite crucible and subsequently heated to 1,050°C for 15 min. The molten sample was then dissolved in 5% HNO_3. Sample solutions were aspirated into an ICP mass spectrometer (Perkin–Elmer Elan 600). The detection limits range from 0.01 to 0.5 ppm. Mineral compositions were determined using a Cameca SX-100 electron microprobe at the Institute of Mineralogy and Petrology in Hamburg (Germany), equipped with five wavelength-dispersive spectrometers. Analytical conditions are 15 kV accelerating voltage, 20 nA beam current and 10 to 30 seconds counting time.

Sr and Nd isotopic analyses were performed at the Institute of Geology and Geophysics, Chinese Academy of Sciences (Beijing). Mass analyses were performed with a multi-collector VG354 mass spectrometer. Rb, Sr, Sm and Nd concentrations were measured using the isotopic dilution method. $^{87}Sr/^{86}Sr$ ratios were normalized against $^{86}Sr/^{88}Sr = 0.1194$. $^{143}Nd/^{144}Nd$ ratios were normalized against $^{146}Nd/^{144}Nd = 0.7219$. $^{87}Sr/^{86}Sr$ ratios were adjusted to NBS-987 Sr standard = 0.710250 and $^{143}Nd/^{144}Nd$ ratios to La Jolla Nd standard = 0.511860. The uncertainty in concentration analyses by isotopic dilution is $\pm$2% for Rb, $\pm$0.4–1% for Sr, and $< \pm$0.5% for Sm and Nd depending upon concentration levels. The overall uncertainty for Rb/Sr is $\pm$2% and Sm/Nd $\pm$0.2–0.5%. Procedural blanks are: Rb = 120 pg, Sr = 200 pg and Nd = 50–100 pg. The detailed analytical procedure for Sr and Nd isotopic measurements are given in Qiao (1988). For Pb isotope analyses, sample powder was spiked and dissolved in concentrated HF for 72 h. Lead was separated and purified by conventional anion-exchange technique with diluted HBr. Isotopic ratios were measured using the VG354 mass spectrometer at the Institute Geology and Geophysics, Beijing.

$^{40}Ar/^{39}Ar$ incremental heating experiments were carried out in the Geochronology Laboratory at the Vrije University. For each sample ca. 200 mg of washed groundmass was packed in 20 mm diameter Al-foil packages and stacked with packages containing a mineral standard into a 23 mm OD quartz tube. The mineral standard is DRA-1 sanidine (with a K/Ar age of 25.26 Ma). The quartz vial was packaged in a standard Al-irradiation capsule and irradiated for 1 h in a Cd-lined rotating facility (RODEO) at the NRG-Petten HFR facility in The Netherlands. Laser incremental heating was carried out using a Synrad 48-5 CO_2 laser. A typical mass spectrometer run consists of stepping through the argon mass spectrum. Details of the analytical method were described by Wijbrans et al. (1995).

Results

Sample description

Host rocks

Most rocks from these plutons are medium-grained (Fig. 2a), containing plagioclase grains that display oscillatory zoning and sieve textures ($\sim$20 mm; Fig. 2b), characteristics that can be attributed to magma mixing (e.g., Vernon 1990; Hibbard 1991; Waight et al. 2000) in a finer-grained matrix of plagioclase (20–70%), quartz

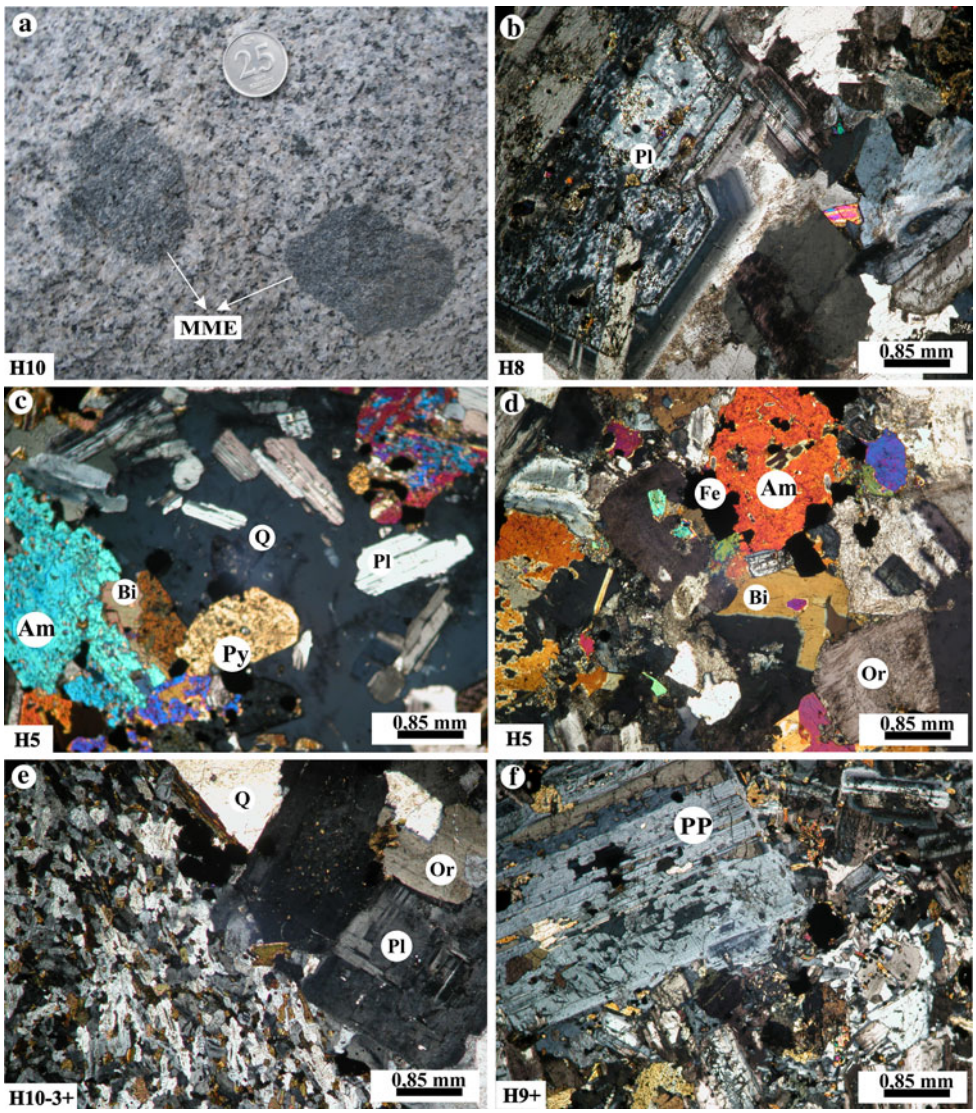

Fig. 2 **a** Macroscopic view of mafic microgranular enclaves within the host rocks and **b–f** photomicrograph showing textural relationships of the host granitoid rocks and their enclaves. The features are amphibole (*Am*), plagioclase (*Pl*), biotite (*Bi*), quartz (*Q*), orthoclase (*Or*), pyroxene (*Py*), Fe–Ti oxides (*Fe*) and plagioclase phenocryst (*PP*)

(3–40%), K-feldspar (4–45%), amphibole (1–25%), biotite (0–15%), pyroxene (cpx; 0–8%) and iron–titanium oxides (1–5%), in descending order of abundance. Mafic constituents are represented by amphibole, biotite and pyroxene, with amphibole prevailing in abundance over biotite and pyroxene (Fig. 2c, d). Dioritic rocks contain amphibole and biotite (amphibole > biotite) in abundances greater than that found in granitic, granodioritic and tonalitic rocks. A lath-shaped plagioclase is commonly observed. Plagioclase ranges in composition from An_{67} to An_{28}, with Or content is smaller than 1 mol.% (Supplementary Table 1). Orthoclase ($Or_{95–75}Ab_{2–25}An_{1–0}$) contains finer-grained plagioclase, amphibole and biotite. Quartz is anhedral and poikilitic and includes finer-grained plagioclase, biotite, amphibole and pyroxene (Fig. 2c). Green to brownish-green amphiboles are generally anhedral, with inclusions of Fe–Ti oxide and apatite (Fig. 2d). Amphiboles are generally calcic and characterized by X_{Mg} [=Mg/(Mg + Fe_{tot})] = 0.57–0.72 (Supplementary Table 2). Biotite forms large subhedral to euhedral crystals and has variable TiO_2 content (4.08–5.62 wt%) and X_{Mg} of 0.52–0.61 (Supplementary Table 3). Pyroxene occurs as small, yellowish green subhedral grains (~2 mm) (Fig. 2c, d). Augitic pyroxenes have X_{Mg} ranging from 0.74 to 0.80. Fe–Ti oxides coexist with mafic silicates. Large titanomagnetite ($Mt_{97–72}Usp_{28–03}$) is surrounded by finer-grained ilmenite ($Ilm_{98–67}Hm_{33–02}$) (Supplementary Table 4). Apatite is present as irregular blobs within titanomagnetite, biotite, amphibole and plagioclase. Sphene is concentrated around large titanomagnetite grains. Zircon is an accessory phase in all rock types and occurs as prismatic crystals.

Mafic microgranular enclaves

Mafic microgranular enclaves (MME) are widespread within the plutons, but their spatial distribution is heterogeneous.

When compared to the host rocks, the MMEs are fine-grained and gabbroic diorite in composition. They have ellipsoidal and flattened shapes. These features suggesting plastic behavior at the moment of their incorporation into the hybrid host magma are due to their plastic rheology (Frost and Mahood 1987; Poli and Tommasini 1991). The MMEs are commonly 1 mm to 1 m in size (Fig. 2a). Their contacts with their host are sharp, rounded or irregular, and big enclaves have diffusive contacts without deformation, a characteristic that can be attributed to the undercooling and mingling of hybrid MME globules formed by a mixture of mafic and felsic magmas (e.g., Perugini et al. 2003). The degree of thermal, rheological and compositional contrast of co-existing mafic and felsic magmas governs the hybridization levels, preserving the megascopic features (mafic microgranular enclaves) relevant to the magma mixing (e.g., Kumar et al. 2004). The MMEs show magmatic textures similar to the poikilitic-equigranular textures of basic igneous rocks. In addition, no cumulate textures are found in the MMEs. The MMEs contain higher ferromagnesian phases, plagioclase, lower quartz and K-feldspar than those of the host rocks (Fig. 2e, f). They are composed of plagioclase (55–70%), amphibole (5–15%), biotite (3–15%), pyroxene (1–5%), orthoclase (2–6%), quartz (2–9%) and Fe–Ti oxides (1–3%) and also contain sieve and large plagioclase crystals (Fig. 2f). In some cases, large felsic minerals crosscut the enclave/host boundary. These features, common in enclaves worldwide, are considered to indicate a liquid state of the enclaves upon their incorporation into the more felsic magma (e.g., Vernon 1984; Perugini et al. 2003). In addition, the host rock's mafic xenocrysts are absent within the MMEs, while titanomagnetite is always present. Small ilmenites and acicular apatites also occur as accessories. The presence of acicular apatite and quartz ocelli reflect on the hybridization process associated with the generation of the MMEs.

^{40}Ar–^{39}Ar dating

In this study, new radiometric age data has been generated by the ^{40}Ar/^{39}Ar incremental heating method on the hornblende separate (sample; H5). The sample yielded a good plateau over 80% of the gas release. The dispersion in the sample along the isochron line was poor. It yielded in this respect the best results, with reasonable enrichment in radiogenic argon and good agreement between plateau and isochron ages. Consequently, the plateau age was considered to be the more reliable estimate of the age. Results of the present dating work are given in Table 1, and Fig. 3 shows the results in the form of age spectra. ^{40}Ar/^{39}Ar dating of a hornblende separate from the pluton yielded a plateau age of 79.70 ± 0.75 Ma. The hornblende age corresponds to the time of hornblende cooling to its blocking temperature, at about 525 ± 25°C (e.g., Harland et al. 1990). In addition, the sample is fresh and expected to give reliable ages to represent the cooling histories of the plutons. Therefore, the hornblende cooling age of ~79 Ma (middle Campanian) is interpreted as an approximation for the intrusion age. The intrusion has cut the subduction-related Cenomanian–Turonian aged volcano sedimentary rocks of Çağlayan Formation.

Major and trace elements

Data on major and trace elements of the Harşit pluton are listed in Table 2. In the classification diagram of

Table 1 ^{40}Ar/^{39}Ar dating values for the Harşit sample from the Eastern Pontides

Sample no/step (H5)	Incremental heating (w)	$^{40}Ar_{(K)}$ (%)	$^{39}Ar_{(K)}$ (%)	K/Ca ± 2σ	^{40}Ar/^{36} Ar(i) ± 2σ	Weighted plateau [age ± 2σ (Ma)]
1	6	8.29	0.27	0.182 ± 0.010	322.2 ± 8.0	125.30 ± 33.09
2	7	11.32	0.38	0.128 ± 0.007	333.2 ± 8.3	105.11 ± 19.90
3	8	15.59	0.58	0.078 ± 0.004	350.1 ± 8.6	88.52 ± 11.57
4	7	33.26	4.15	0.046 ± 0.002	442.8 ± 11.1	92.78 ± 4.60
5	8	46.65	7.13	0.046 ± 0.002	553.9 ± 14.1	84.91 ± 2.48
6	9	50.33	7.81	0.048 ± 0.003	595.0 ± 14.9	81.78 ± 2.04
7	17	75.08	30.14	0.051 ± 0.003	1185.9 ± 33.0	81.30 ± 0.90
8	22	77.87	25.29	0.053 ± 0.003	1335.9 ± 37.5	80.68 ± 0.80
9	27	84.30	19.97	0.061 ± 0.003	1882.8 ± 30.5	79.38 ± 0.29
10	25	92.25	4.26	0.138 ± 0.008	3770.1 ± 176.8	79.30 ± 0.58

Plateaus ages were calculated over concordant steps (as defined by the MSWD value calculated for the plateau steps), the percentage of the gas release included in the plateau calculation is given in the column $^{40}Ar_{(K)}$ and $^{39}Ar_{(K)}$, the number of steps forming the plateau is *n*. 40/36(i) refers to the non-radiogenic intercept ratio of ^{40}Ar/^{36}Ar, which are in all cases indistinguishable from the value for modern air. Isochron ages were calculated over the steps that represent the plateau. Errors given are ±2σ. Ages were calculated on the basis of an age for the laboratory Standard sanidine DRA-1 of 25.26 ± 0.2 Ma

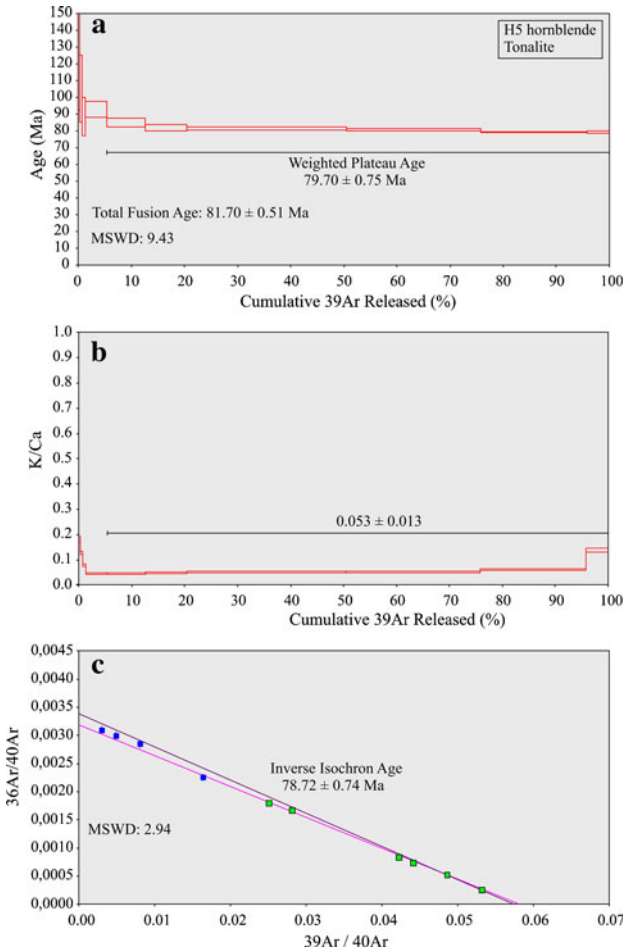

Fig. 3 Apparent age and K/Ca spectra and inverse isochron plot of hornblende from the Harşit pluton by incremental heating

Middlemost (1994), the host rocks from the pluton plot in the fields of granite, granodiorite, tonalite and diorite, and their MMEs in the fields of only gabbroic diorite (Fig. 4). The host rocks are metaluminous to slightly peraluminous with ASI [=molar $Al_2O_3/(CaO + K_2O + Na_2O)$] ranging from 0.84 to 1.04. They are of I-type character, while the MMEs are only metaluminous (ASI = 0.79–0.83) (Fig. 5a, b). All the samples exhibit a high-K calc-alkaline compositional trend (Fig. 5c). They are close to the boundary marked by the line $\sigma = 2.5$, also suggesting the presence of high-K calc-alkaline character (Fig. 4). The major element characteristics of the Harşit pluton are typical of metaluminous, K-rich calc-alkaline granitoids (KCG) according to classification of Barbarin (1999). The variation of selected major and trace elements is shown in Fig. 6. The host rocks display a wide range in SiO_2 content and low Mg# (59–76%, Mg# = 11–46), but the MMEs are less differentiated than the host rocks (with SiO_2 = 54–56%, Mg# = 45; Table 2). All of the rocks define a similar variation trend without a compositional gap in most of the Harker plots (Fig. 6a–i), suggesting that low-pressure fractional crystallization (LPFC), rather than high-pressure fractional crystallization (HPFC), is the significant magmatic process in the evolution of the rocks. All of the samples exhibit similar trace element abundance patterns, with enrichment in large ion lithophile (LIL) elements (e.g., Rb, Th, K and Ba) and pronounced negative anomalies in high field strength (HFS) elements such as Ti and Nb compared to N-MORB (Fig. 7a). Chondrite-normalized REE patterns are plotted in Fig. 7b. The REE abundance patterns of the samples are all characterized by a fractionation between light and heavy REEs. The host rocks and their enclaves display rather similar fractionated REE pattern, with weaker concave-upward patterns of heavy REEs than their mafic enclaves (Fig. 7b). They have a narrow range of Eu/Eu* ratios (0.30–0.76; Table 2) and have small negative Eu anomalies (host rocks; Eu/Eu* = 0.30–0.76, MMEs; Eu/Eu* = 0.57–0.67), probably resulting from fractional crystallization of plagioclase during magma evolution. The Harşit pluton is characterized by very low abundances of HFS elements (Nb, Hf and Zr; e.g., Nb < 11 ppm).

Sr–Nd–Pb isotopes

Whole-rock Sr, Nd and Pb isotopic data for the Harşit pluton are reported in Tables 3 and 4. Samples were selected in such a way that covers the entire range of the compositional spectrum of the host rocks and mafic enclaves, from the most primitive rock types to the most evolved ones. Initial Nd–Sr isotopic compositions were calculated at an age of 79 Ma. Regardless of rock types and SiO_2 content, the host rocks from Harşit plutons display relatively homogeneous isotopic compositions of I_{Sr} (79 Ma) ranging from 0.70676 to 0.70708 and of ε_{Nd} (79 Ma) from −3.3 to −4.4. The corresponding Nd model ages (T_{DM}) are in the range of 1.05–1.22 Ga. The MMEs show I_{Sr} (79 Ma) (0.70686–0.70694) and ε_{Nd} (79 Ma) values (−3.9 to −4.0) similar to their respective host rocks, but the Nd model ages (T_{DM} = 1.21–1.36 Ga) are slightly older than those of the host rocks. All samples have a negative correlation between both parameters, whereby ε_{Nd} (79 Ma) decreases with increasing I_{Sr} values.

As illustrated in Fig. 8, the samples mostly plot in the right quadrants of a conventional Sr–Nd isotope diagram. There, they define a trend similar to the Eastern Pontide lower crustal-derived adakitic granitoid (Topuz et al. 2005), hybrid granitoids from the eastern Pontide (Karsli et al. 2007), Central Anatolian lower crustal-derived adakitic volcanics (Varol et al. 2007) and the subduction-related plagioleucitites (Altherr et al. 2008), but they do not overlap the fields cited. The samples plot near the field of early Cenozoic adakitic volcanic rock (Karsli et al. 2010) and the subduction-related Campanian high-K trachyandesites (Eyüboğlu 2010). They have much lower ε_{Nd} (t)

Table 2 Major oxide and trace element analyses of the Harşit plutonic rocks from the Eastern Pontides

Sample Rock type	H3 gr	H4 tn	H5 tn	H6 tn	H8 tn	H9 tn	H10 tn	H12 tn	H13 grd	H14 dio	H9+ gbb.dio	H10-3+ gbb.dio
SiO_2	76.95	62.53	63.69	63.37	62.85	63.12	61.24	62.21	69.52	59.43	56.32	54.95
TiO_2	0.06	0.49	0.48	0.49	0.50	0.49	0.52	0.53	0.37	0.62	0.71	0.66
Al_2O_3	12.39	15.62	15.41	15.33	15.48	15.69	16.04	15.61	14.35	16.02	16.65	16.33
$Fe_2O_3^{tot}$	1.86	5.93	5.61	5.80	5.95	5.68	6.30	5.95	3.68	7.28	8.70	9.84
MnO	0.02	0.13	0.10	0.11	0.09	0.09	0.12	0.11	0.05	0.11	0.13	0.19
MgO	0.12	2.28	2.14	2.28	2.34	2.20	2.46	2.39	1.02	3.18	3.64	4.03
CaO	1.00	5.14	4.99	5.07	5.23	4.98	5.70	5.34	2.95	6.46	6.69	7.59
Na_2O	4.20	2.80	2.83	2.68	2.75	2.71	2.67	2.81	2.79	2.87	2.82	2.66
K_2O	2.96	3.93	3.78	3.92	3.84	3.77	3.78	3.48	4.34	2.47	3.04	2.31
P_2O_5	0.01	0.11	0.12	0.12	0.13	0.13	0.13	0.14	0.06	0.13	0.17	0.13
LOI	0.30	0.90	0.70	0.70	0.70	1.00	0.90	1.30	0.70	1.30	1.00	1.20
Total	99.87	99.86	99.85	99.87	99.86	99.86	99.86	99.87	99.83	99.87	99.87	99.89
Mg#	0.11	0.43	0.43	0.44	0.44	0.43	0.44	0.44	0.35	0.46	0.45	0.45
ASI	1.04	0.86	0.87	0.86	0.85	0.89	0.85	0.86	0.98	0.84	0.83	0.79
Rb	65	120	117	135	126	110	129	110	129	80	103	92
Sr	78	314	326	317	330	319	359	330	197	308	361	346
Ba	477	859	1004	902	1003	1083	1018	936	1408	920	951	583
Cs	0.6	1.8	2.5	3.7	3.1	1.7	2.0	4.0	0.8	1.4	2.2	2.2
Zr	134	157	140	129	147	149	122	128	155	125	102	39
Hf	4.6	4.9	4.5	4.1	4.7	4.6	3.8	3.9	5.2	3.8	3.1	1.8
Ta	0.4	0.8	0.6	0.8	0.7	0.6	0.6	0.6	0.8	0.5	0.7	0.6
Th	9	24	19	20	21	17	19	18	22	12	15	15
Nb	5	11	9	11	10	9	9	9	11	8	10	11
Pb	6	8	7	14	8	12	12	14	13	10	10	15
Y	21	27	24	25	26	24	24	25	25	26	29	32
Ga	12	16	16	15	16	16	16	15	14	17	18	18
Ni	9	8	5	5	5	11	5	6	6	5	7	9
Co	10	13	13	14	14	14	16	15	7	17	23	27
V	5	137	132	140	147	132	159	141	64	200	222	259
Zn	9	21	16	28	13	22	27	28	22	15	26	42
La	17.31	26.61	32.51	29.51	33.74	31.21	29.02	26.03	42.82	26.82	28.02	19.52
Ce	41.50	57.90	64.03	59.72	65.91	61.91	58.71	55.22	83.23	53.33	59.51	47.02
Pr	4.77	6.61	6.69	6.37	6.69	6.41	6.16	6.11	8.09	5.76	6.69	5.94
Nd	19.02	24.54	24.11	22.40	23.91	23.30	21.52	23.03	26.74	20.93	24.90	23.52
Sm	4.91	4.52	4.23	4.11	4.22	3.92	4.11	4.32	4.38	4.07	4.88	5.06
Eu	0.52	0.88	0.95	0.93	0.89	0.95	0.94	0.92	0.86	1.00	1.06	0.93
Gd	5.66	4.27	3.69	3.72	3.97	3.67	3.80	3.96	3.80	3.94	4.76	4.89
Tb	1.09	0.75	0.66	0.68	0.72	0.68	0.67	0.71	0.69	0.72	0.87	0.92
Dy	6.32	3.89	3.52	3.61	3.71	3.47	3.33	3.46	3.43	3.95	4.52	4.69
Ho	1.43	0.75	0.64	0.71	0.71	0.69	0.64	0.73	0.67	0.73	0.83	0.90
Er	4.32	2.32	2.00	2.12	2.27	2.03	1.97	2.06	2.15	2.19	2.53	2.76
Tm	0.71	0.35	0.32	0.34	0.34	0.32	0.31	0.33	0.33	0.34	0.41	0.42
Yb	4.85	2.42	2.12	2.35	2.34	2.14	2.05	2.10	2.32	2.23	2.57	2.65
Lu	0.70	0.39	0.33	0.40	0.37	0.35	0.33	0.35	0.38	0.35	0.39	0.42
$(La/Yb)_n$	2.40	7.41	10.34	8.46	9.71	9.83	9.54	8.35	12.44	8.10	7.35	4.96
Eu/Eu*	0.30	0.61	0.73	0.72	0.66	0.75	0.72	0.68	0.64	0.76	0.67	0.57

ASI is the aluminium saturation index [molar $Al_2O_3/(CaO + K_2O + Na_2O)$]. Mg# is $100 \times MgO/(MgO + 0.9FeO_{tot})$ in molar proportions. Oxides are given in wt%, trace elements in μg/g

Rock types: *gr* granite, *grd* granodiorite, *tn* tonalite, *dio* diorite, *gbb.dio* gabroic diorite, + mafic microgranular enclave

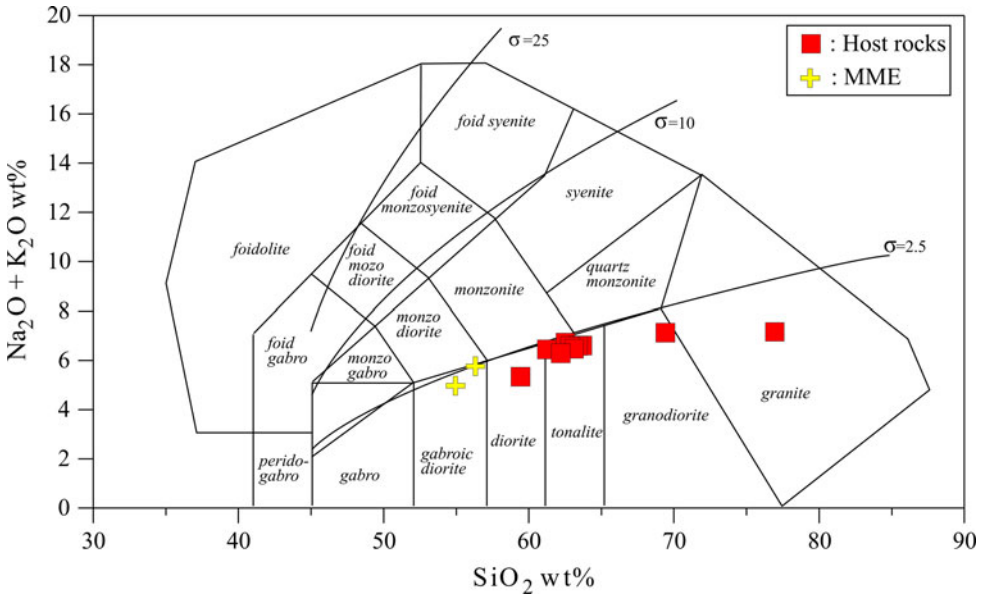

Fig. 4 Classification diagram (Middlemost 1994) for the Harşit pluton. σ is a Rittmann index, defined as $(K_2O + Na_2O)^2/(SiO_2 - 43)$

than those of 400–179 Ma MORB (Mahoney et al. 1998; Xu et al. 2003; Xu and Castillo 2004) and Cenozoic adakites formed by slab melting (Defant et al. 1992; Kay et al. 1993; Sajona et al. 2000) (Fig. 8).

The Harşit samples display limited ranges of $^{206}Pb/^{204}Pb$, $^{207}Pb/^{204}Pb$ and $^{208}Pb/^{204}Pb$ isotopic ratios. Lead isotopic ratios of the samples are $^{206}Pb/^{204}Pb = 18.79–18.87$, $^{207}Pb/^{204}Pb = 15.59–15.61$, $^{208}Pb/^{204}Pb = 38.71–38.83$. The northern hemisphere reference line (NHRL; Hart 1984) was used in the plots, since ^{208}Pb data are more radiogenic than ^{206}Pb and plot well above the NHRL in conventional Pb isotope diagrams (Fig. 9a, b). Also plotted for comparison are EM1 and EM2 (Zindler and Hart 1986). All the samples are homogeneous in lead isotopic compositions (Fig. 9a, b). The fields of the Dölek and Sariçiçek plutons (DSP) and the Quaternary Erzincan Volcanics (QEV) are shown for reference. All of the samples plot in the field of the lower crust and closer to the field of the QEV. They are far from EM1 and are not EM2 end-members (Fig. 9a, b).

Discussion

Petrogenetic considerations of the high-K calc-alkaline rocks

The hybrid host rocks from the Harşit pluton are dominated by granite, tonalite, granodiorite and dioritic rocks. The origin of the high-K calc-alkaline rocks has been the subject of many studies, and two main models have been proposed to interpret their petrogenesis: (1) pure crustal melts from partial melting of mafic lower crust at relatively high pressures (e.g., Roberts and Clemens 1993; Liu et al. 2002) or (2) evolution of a mixture of crustal- and mantle-derived magmas (e.g., Barbarin 1999; Ferré and Bernard 2001; Chen et al. 2003; Yang et al. 2007). All of the data in this work favor the second model, in which a magma mixing process can better explain the genesis of the rocks. The causes of the geochemical variation within the pluton were investigated using binary diagrams and Sr–Nd isotopic modeling. The principal evidence for this generation model is described below.

Fractional crystallization

A wide variety of rock types were most likely generated by fractional crystallization, which is a probable mechanism to explain the generation of the samples, as argued below. The proportions of Al_2O_3, MgO, CaO, $Fe_2O_3^{tot}$ and La decrease and those of ASI, K_2O and Ba increase with increasing SiO_2, suggesting fractionation dominated by amphibole and calcic plagioclase (Figs. 5a, 6a, c, d, e, f, h, i). Depletion in HREE, Zr and Y can be related to the fractionation of zircon. The negative correlations of CaO, $Fe_2O_3^{tot}$ and MgO with SiO_2 may also reflect on pyroxene fractionation. The host rocks and their MMEs are characterized by high CaO and Sr contents and have small Ba, Sr and Eu negative anomalies (Fig. 7a, b), suggesting that plagioclase fractionation has played a role in their genesis. These geochemical features, along with the mineralogy, are consistent with a genetic relationship between the least and most evolved products of the pluton.

The fractional crystallization process for the pluton was modeled by a least-squares method for the major elements. The compositions of plagioclase, amphibole, biotite and Fe–Ti oxides used in the models are derived from microchemical analyses of minerals from the rocks of the pluton. The calculations were based on the average composition of

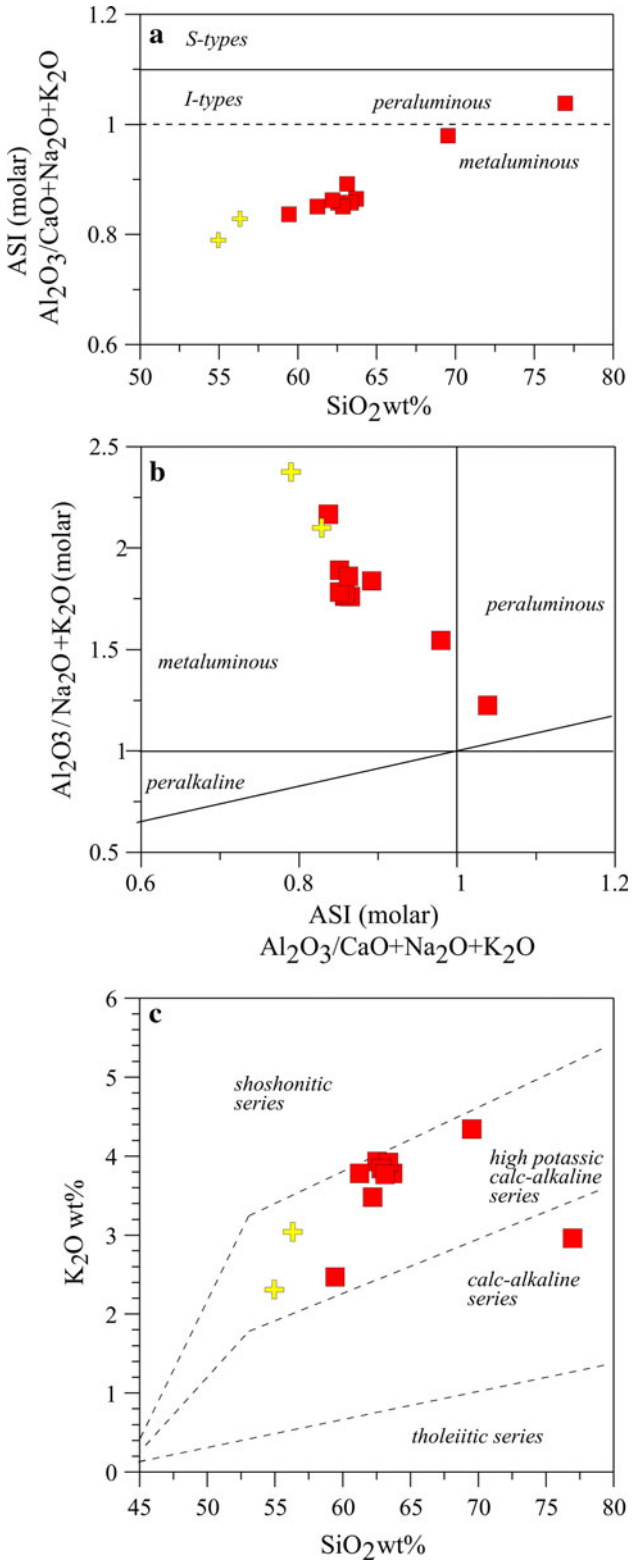

◀ **Fig. 5** Chemical variation diagrams for the Harşit pluton illustrating some chemical features that distinguish between the granitoid rocks. **a** ASI versus SiO_2 diagram. **b** $Al_2O_3/Na_2O + K_2O$ (molar) versus ASI (after Maniar and Piccoli 1989) diagram for the pluton. **c** K_2O versus SiO_2 diagram for the samples with lines separating tholoiitic, calc-alkaline, high-K calc-alkaline and shoshonitic series of Peccerillo and Taylor (1976)

the gabbroic diorite (MME) and used diorite as the parent and diorite and granite as the daughter from the pluton. Two stages of the crystal fractionation were calculated: (1) formation of diorite (host rock) from gabbroic diorite (MME); (2) formation of tonalite from diorite. The results of these calculations are given in Table 5. Most solutions represented here have sums of squared residuals less than 1. The first calculation (stage 1) demonstrates that dioritic host rocks could be produced from the parent magma by fractionation of 8% plagioclase, 3% amphibole, 5% biotite and 2% magnetite. The proportion of the melt remaining is 80 wt%. To produce the tonalite daughter from the diorite magma (stage 2), extractions of lesser amounts (in total of ~28 wt%) of plagioclase, amphibole, biotite and Fe–Ti oxides are necessary (Table 5). For stages 1 and 2, the residual sums of squares are 0.15 and 0.14, respectively, implying that the crystallizing mineral phases and their proportions were reasonably predicted. The proportion of minerals fractionated seems realistic, considering the modal mineral composition of the rocks. The fractionation modeling shows that crystal fractionation is a plausible mechanism to produce a wide variety of rock types from the Harşit pluton. The effects of assimilation may be assessed by elemental and isotopic ratios. The weak correlation appears between ε_{Nd} (79 Ma) and I_{Sr} (79 Ma) and SiO_2 content (Fig. 6j, k), suggesting assimilation plays minor role in the generation of the rocks.

Magma mixing process

The mixing process is supported by the presence of disequilibrium textures such as sieve and oscillatory plagioclases in the host rocks (Fig. 2b). The existence of widespread MMEs points to a mixing process for their genesis. As described above, the MMEs are not cognate fragments of cumulate minerals and refractory "restite" from source-rock anatexis. Therefore, at least two separate magmas are required to explain their generation. The mixing process is consistent with the significant overlap of the data points of the host rock and their MMEs in ε_{Nd} (79 Ma) versus I_{Sr} (79 Ma) plot (Fig. 8). Furthermore, the plots of the isotopic variations against the elemental compositions are attributed to magma mixing (e.g., Thirlwall and Jones 1993; Chen et al. 2002; Chen and Arakawa 2005).

Whenever a magma-mixing scenario was invoked, it was quantified by a mixing test using Sr–Nd isotopic modeling. The principle of this test is that all of the Sr–Nd isotopic compositions of the samples that originated by magma mixing should plot on a straight line between two end-members in a diagram of I_{Sr} ratios versus ε_{Nd} (t). In the

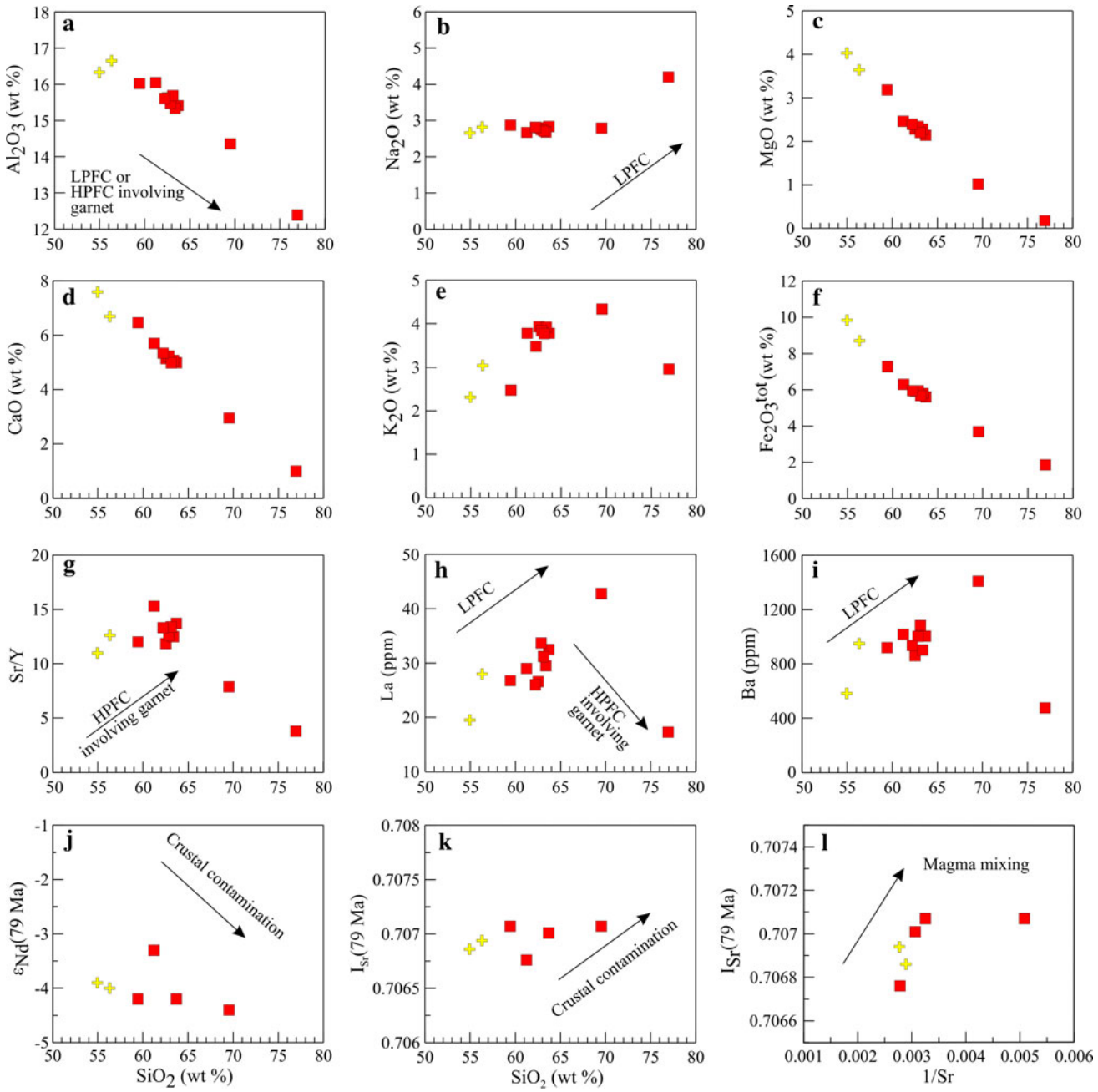

Fig. 6 **a** SiO_2 versus Al_2O_3; **b** SiO_2 versus Na_2O; **c** SiO_2 versus MgO; **d** SiO_2 versus CaO; **e** SiO_2 versus K_2O; **f** SiO_2 versus $Fe_2O_3^{tot}$; **g** SiO_2 versus Sr/Y; **h** SiO_2 versus La; **i** SiO_2 versus Ba; **j** SiO_2 versus ε_{Nd} (79 Ma); **k** SiO_2 versus I_{sr} (79 Ma); **l** 1/Sr versus I_{sr} (79 Ma). *HPFC* high-pressure fractional crystallization involving garnet (Macpherson et al. 2006), *LPFC* low-pressure fractional crystallization involving olivine + clinopyroxene + plagioclase + hornblende + titanomagnetite (Castillo et al. 1999)

modeling, the average parent magma from the isotopically depleted mantle was assumed to represent the mafic end-member. Sample K42b (dioritic enclave) from the Köse pluton described by Dokuz (2009) in the eastern Pontides is assumed to be representative of the magma derived from the local (lower continental) crustal end-member; thus, it should theoretically possess the same isotopic signature as the local lower crust. The Sr–Nd isotopic ratios and trace element concentration data explaining the modeling results are given in Fig. 10. The samples plot on a curve, suggesting a magma mixing process. Concerning the proportions of the incorporated end-members, the modeling results demonstrate that ~65–75% of the lower crust-derived magma may be incorporated with the mantle-derived mafic magma (~25–35%) in the generation of the granitoid rocks. Additionally, in a plot of I_{Sr} (79 Ma)

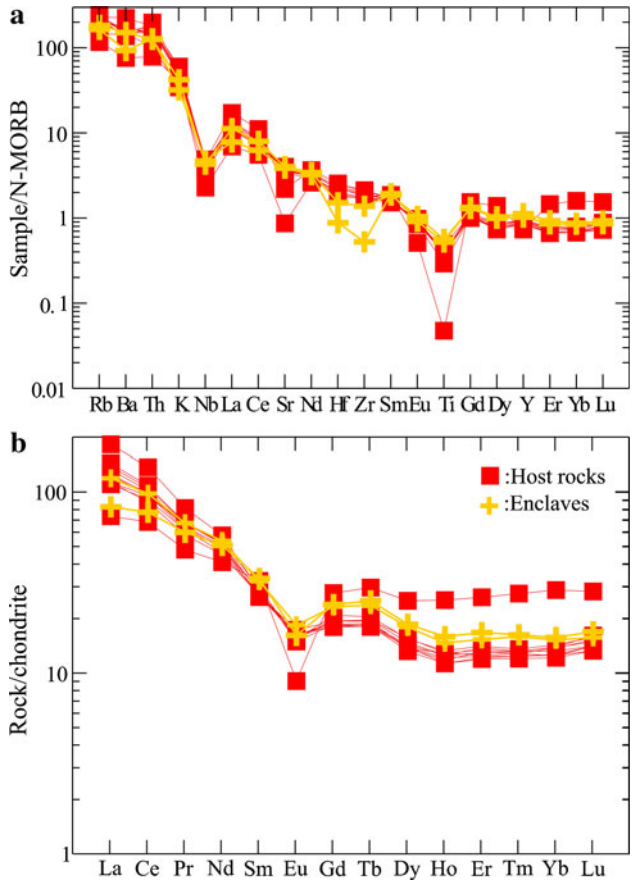

Fig. 7 **a** N-MORB-normalized multi-element variation patterns (normalized to values given in Sun and McDonough 1989) for the Harşit pluton. **b** Chondrite-normalized (to values given in Boynton 1984) rare earth element abundance patterns for the selected samples from the pluton

versus 1/Sr, the MMEs and their host rocks show a linear positive trend, in accordance with a magma mixing process (Fig. 6l).

Source features

The rocks from the Harşit pluton are high-K calc-alkaline and I-type in composition and have a wide range of silica content (SiO_2 = 59–76 wt%) and relatively low Mg# (11–46), both of which indicate that they are not in equilibrium with primary mantle melts. Their Sr–Nd isotope compositions preclude their derivation solely from pure mantle melts. Such compositions could be acquired from (1) partial melting of a mantle source (Grove and Donnelly-Nolan 1986; Han et al. 1997; Soesoo 2000), (2) partial melting of the mafic lower crust (e.g., Wolf and Wyllie 1994; Şen and Dunn 1994; Rapp and Watson 1995; Springer and Seck 1997) or (3) mixing of crust and mantle-derived magmas (e.g., Barbarin 1999; Ferré and Leake 2001; Chen et al. 2003; Karsli et al. 2007; Yang et al. 2007), followed by

Table 3 Sr and Nd isotope data for the Harşit plutonic rocks from the Eastern Pontides

Sample	[Rb] ppm	[Sr] ppm	$^{87}Rb/^{86}Sr$	$^{87}Sr/^{86}Sr$	2σm	I_{Sr} (79 Ma)	[Sm] ppm	[Nd] ppm	$^{147}Sm/^{144}Nd$	$^{143}Nd/^{144}Nd$	2σm	ε_{Nd} (0)	ε_{Nd} (*T*) (79 Ma)	$f_{Sm/Nd}$	T_{DM} (Ga)
Host rocks															
H5	117.12	326.33	1.0407	0.708176	14	0.70701	4.22	24.11	0.1059	0.512377	6	−5.1	−4.2	−0.46	1.09
H10	129.02	359.31	1.0412	0.707925	19	0.70676	4.11	21.52	0.1156	0.512426	6	−4.1	−3.3	−0.41	1.12
H13	128.73	196.81	1.8965	0.709198	18	0.70707	4.38	26.74	0.0992	0.512361	8	−5.4	−4.4	−0.50	1.05
H14	80.41	307.51	0.7582	0.707924	15	0.70708	4.07	20.93	0.1177	0.512380	8	−5.0	−4.2	−0.40	1.22
Enclaves															
H9+	102.61	360.93	0.8244	0.707867	15	0.70694	4.88	24.90	0.1185	0.512395	6	−4.7	−4.0	−0.40	1.21
H10-3+	91.92	346.00	0.7703	0.707723	17	0.70686	5.06	23.52	0.1302	0.512406	9	−4.5	−3.9	−0.34	1.36

$\varepsilon_{Nd} = [(^{143}Nd/^{144}Nd)_s/(^{143}Nd/^{144}Nd)_{CHUR} - 1) \times 10{,}000$, $f_{Sm/Nd} = (^{147}Sm/^{144}Sm)_s/(^{147}Sm/^{144}Sm)_{CHUR} - 1$, $(^{143}Nd/^{144}Nd)_{CHUR} = 0.512638$, and $(^{147}Sm/^{144}Sm)_{CHUR} = 0.1967$. The model ages were calculated using a linear isotopic ratio growth equation: $T_{DM} = 1/\lambda \times \ln[1 + ((^{143}Nd/^{144}Nd)_s - 0.51315))/((^{147}Sm/^{144}Nd)_s - 0.2137)]$

Table 4 Lead isotopic analyses for the granitoidic rocks from the Harşit pluton

Sample	$^{206}Pb/^{204}Pb$	RSD%	$^{207}Pb/^{204}Pb$	RSD%	$^{208}Pb/^{204}Pb$	RSD%
Host rocks						
H5	18.837	0.012	15.606	0.013	38.803	0.014
H10	18.792	0.011	15.601	0.013	38.756	0.014
H13	18.867	0.021	15.611	0.023	38.832	0.020
H14	18.857	0.022	15.603	0.036	38.815	0.031
MMEs						
H9+	18.827	0.017	15.591	0.018	38.725	0.020
H10-3+	18.786	0.015	15.594	0.018	38.705	0.017

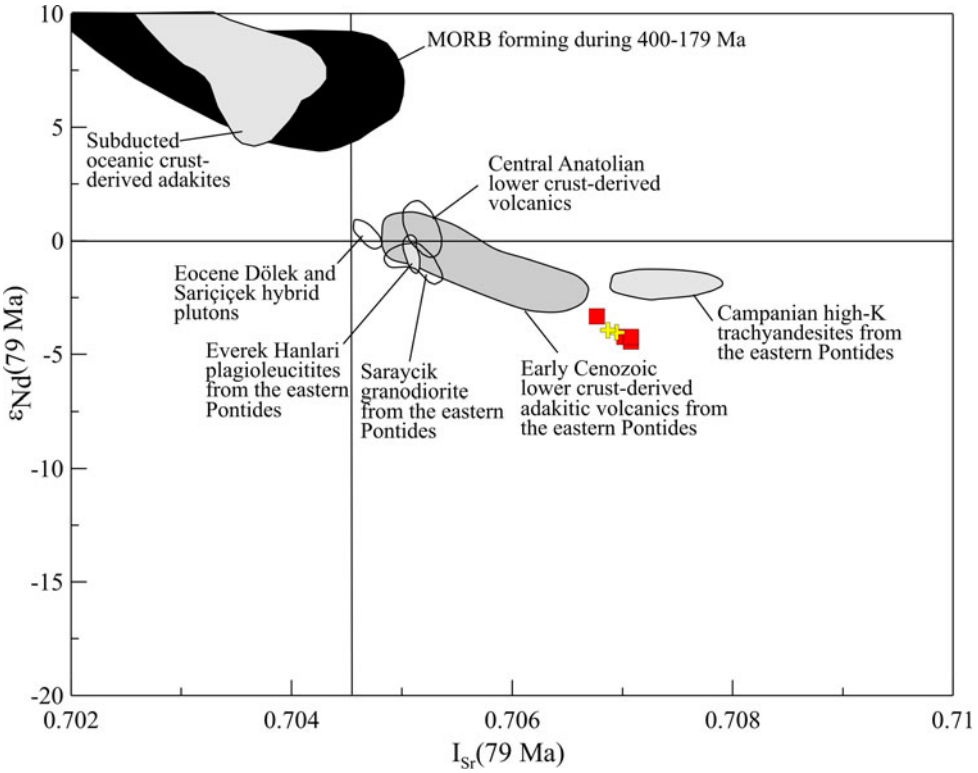

Fig. 8 Nd–Sr isotope compositions of the Harşit granitoid rocks from the Eastern Pontides. Data source are as follows: Cenozoic subducted oceanic crust-derived adakites are after Defant et al. (1992), Kay et al. (1993), Sajona et al. (2000) and Aguillón-Robles et al. (2001); 400–179 Ma MORB are from Mahoney et al. (1998), Xu et al. (2003), Tribuzio et al. (2004) and Xu and Castillo (2004). Central Anatolian lower crustal-derived volcanic fields, Eastern Pontides lower crustal-derived Saraycik granodiorite, Eastern Pontide Paleocene plagioleucitites and Eastern Pontide high-K volcanic rocks were taken after Varol et al. (2007), Topuz et al. (2005), Altherr et al. (2008) and Eyüboğlu (2010), respectively. Eocene Dölek and Sariçiçek hybrid plutons are after Karsli et al. (2007)

fractional crystallization, with or without crustal contamination.

The samples from the pluton are characterized by pronounced negative Ba, Nb and Ti anomalies in the spidergrams (Fig. 7a) and enriched in LILEs and LREEs, suggesting typical crustal melts. However, these features are not always related to the crustal-derived melts, but they point to partial melting of an enriched mantle, which was metasomatized by fluids prior to melting (Hawkesworth et al. 1993; Rottura et al. 1998; Cameron et al. 2003). Most probably, a subcontinental lithospheric mantle source (SCLM) was chemically enriched by fluids rich in LREEs and LILEs or melts derived from the dehydration of the down-going slab containing Paleozoic arc rocks of the earlier tectonic processes modeled by Dokuz et al. (2010) in the region. Lead isotopic ratios of the samples also indicate a minor enriched mantle source (EM2; Fig. 9a, b) that can be considered as an end-member of the mixing process in the genesis. In combined plots of $^{207}Pb/^{204}Pb$ versus $^{206}Pb/^{204}Pb$ and $^{208}Pb/^{204}Pb$ versus $^{206}Pb/^{204}Pb$ (Fig. 9a, b), all of the samples from the Harşit pluton fall within the fields of rocks from the lower crust (LC) described by Kempton et al. (1997) and deviate from the field for samples of the DSP, defined by Karsli et al. (2007). They are closer to the field of the QEVs described by Karsli et al. (2008). Karsli et al. (2007) have suggested a mixed origin for the DSP, involving a SCLM as major and the lower crust as minor components, whereas we propose a mixed origin for the Harşit pluton with lower crustal material as a major component, as is the case in the QEVs from Eastern Turkey. The MMEs have relatively low silica content (55–56%) and relatively high Mg# (>45) that both

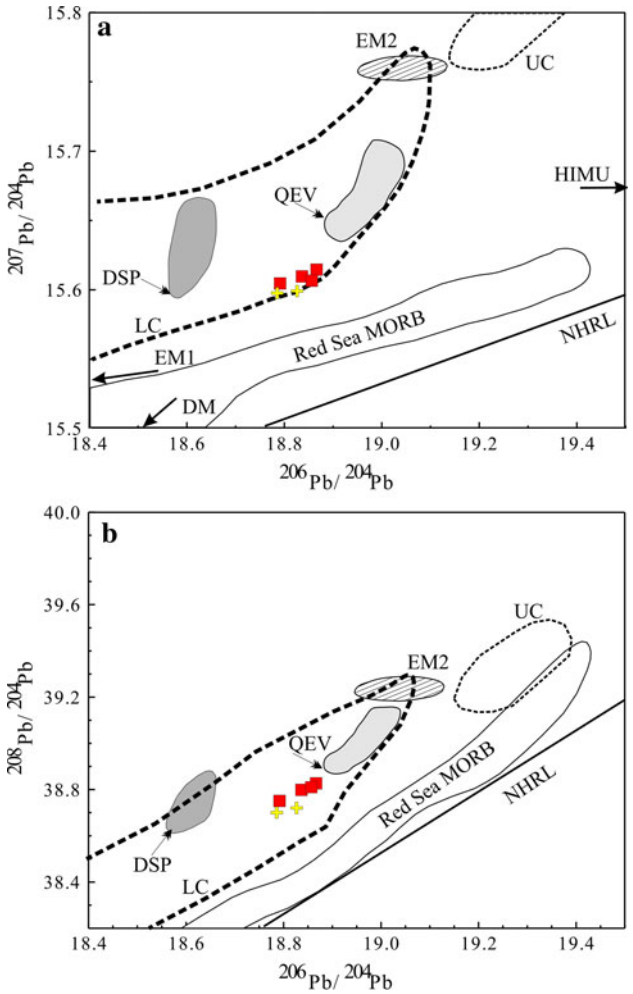

Fig. 9 **a** Plot of plots of $^{207}Pb/^{204}Pb$ versus $^{206}Pb/^{204}Pb$ and **b** $^{208}Pb/^{204}Pb$ versus $^{206}Pb/^{204}Pb$ for the selected samples from the plutons. Field for upper crust (*UC*) and lower crust (*LC*) were taken after Mason et al. (1996) and Kempton et al. (1997), respectively

point to the contribution of a mantle-derived component. The low Ni (6–9 ppm) content of the MMEs relative to those of unfractionated magmas (200–450 and >1,000, respectively) suggests that a mafic magma underwent significant fractionation of olivine, pyroxene and spinel prior to the magma mixing. However, the Al_2O_3 content (16.33 wt%) is not consistent with basic parent melts ($Al_2O_3 < 15$ wt%) in equilibrium with the mantle source, a discrepancy that is probably due to the fractionation of some Al-poor mafic phases such as olivine and orthopyroxene. Thus, it appears unlikely that felsic magmas were derived from basaltic parent magma by fractional crystallization or an AFC process, because the host rocks have SiO_2 content >56 wt% and none of them are of early differentiated, more basaltic composition in the area. This observation weakens the possibility of generation from a pure basaltic magma by fractional crystallization.

Alternatively, partial melting of the mafic lower crust could have produced the Harşit rocks. Wyllie and Wolf (1993), Wolf and Wyllie (1994), and Lopéz and Castro (2001) showed experimentally that amphibolites start to melt at relatively high temperatures (800–900°C) at pressures <1 GPa, whereas at ~1 GPa, dehydration melting commences at temperatures as low as 750°C. In addition, the melt composition resulting from the partial melting of the mafic lower crust is controlled by the water content, source composition, degree and *P–T* conditions of the melting (e.g., Rapp et al. 1991; Sen and Dunn 1994; Wolf and Wyllie 1994; Rapp and Watson 1995; Winther 1996; Lopéz and Castro 2001). Recent experimental data have shown that regardless of the degree of partial melting, the partial melting of the mafic lower crust also could generate melts of metaluminous granitic composition (e.g., Rushmer 1991; Tepper et al. 1993; Roberts and Clemens 1993; Wolf and Wyllie 1994; Rapp and Watson 1995). The most felsic sample, H3, is characterized by high silica (~76 wt%) and relatively low Mg# (11), while the evolved samples have higher I_{Sr} (79 Ma) (0.70707), all of which would be consistent with melts derived from the lower crust. In contrast, the most primitive sample, H14, has a silica content of ~59 wt% and Mg# = 45. If the source magma was derived directly from partial melting of mafic rocks in the lower crust, the Harsic rocks should have relatively low MgO content, similar to experimental melts of Rapp and Watson (1995). This is not the case in the Harşit samples (Table 2). In contrast with experimentally derived melts, the samples have low $Al_2O_3/(FeO + MgO + TiO_2)$ and high $Al_2O_3 + FeO + MgO + TiO_2$ values and plot in the field of amphibolite-derived melts (Fig. 11). In light of all these data, the most likely scenario is that a mafic, amphibole- and plagioclase-bearing lower crust underwent dehydration melting, playing an important role (~75%) as a more felsic component in the generation of the hybrid Harşit samples.

As discussed above, the most likely interpretation for the generation of the Harşit rocks is that they represent a mixture of two end-members derived from SCLM and the lower crust is. That is, the parent magma of the entire intermediate rock spectrum is in fact a hybrid magma that subsequently underwent a fractionation process rather than a magma-derived process purely from the lower crust. For a more mafic end-member, the SCLM-derived magma seems less likely because of the relatively low initial Sr–Nd isotopic ratios of the hybrid granitoid rocks. The MMEs from the pluton, with their finer grain sizes attributed to the undercooling of a mafic magma in a cooler, felsic magma (e.g., Vernon 1984; Wiebe 1991; Barbarin and Didier 1992; Perugini and Poli 2000; Kumar et al. 2004), have mineral assemblages, chemical relationships and isotopic compositions similar to their host rocks. The MMEs contain large, rounded plagioclase phenocrysts, which are

Table 5 Major element oxides fractional crystallization modeling for the rocks from the Harşit pluton

	Stage 1: Gabbroic diorite–Diorite			Stage 2: Diorite–Tonalite		
	Parent Average ($n = 2$)	Daughter Observed ($n = 1$)	Calculated	Parent Average ($n = 1$)	Daughter Observed ($n = 7$)	Calculated
SiO_2	55.64	59.43	60.44	59.43	62.72	64.60
TiO_2	0.69	0.62	0.80	0.62	0.50	0.31
Al_2O_3	16.49	16.02	16.37	16.02	15.60	15.60
FeO^t	9.27	7.28	7.45	7.28	5.89	5.09
MgO	3.84	3.18	3.31	3.18	2.30	2.14
CaO	7.14	6.46	6.51	6.46	5.21	5.14
Na_2O	2.74	2.87	2.67	2.87	2.75	2.93
K_2O	2.68	2.47	2.33	2.47	3.79	4.14
P_2O_5	0.15	0.13	0.08	0.13	0.13	0.08
Fractionating	Plagioclase		8.55			16.26
Minerals (wt%)	Amphibole		3.71			10.18
	Biotite		5.23			–
	Magnetite		2.14			2.35
Residual melt (wt%)			80.37			71.21
Sum residuals squared	r^2		0.15			0.14

Major elements are recalculated to total = 100% volatile free, total Fe as FeO. Mineral compositions used for modeling are an average value of mineral compositions given in Supplementary Tables 1, 2, 3 and 4

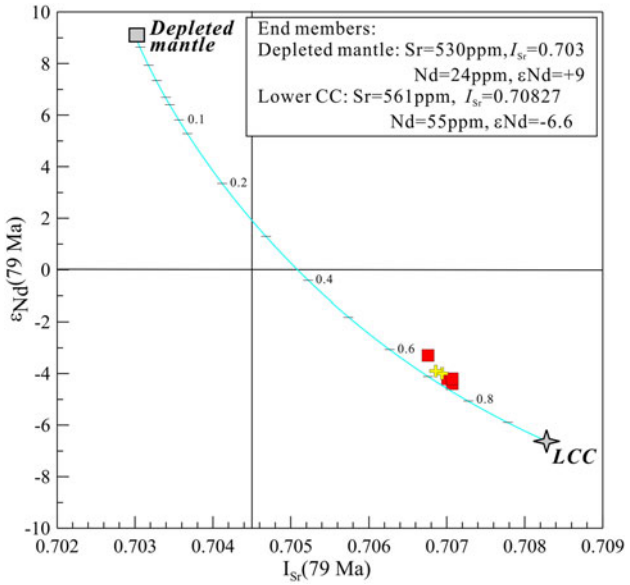

Fig. 10 A simple modeling diagram showing a trend of Sr–Nd isotope variation as a result of magma mixing

texturally similar to those in the host rocks (Fig. 2f). Karsli et al. (2007) showed that plagioclase crystals of MME are chemically similar to those of the host rocks in closest proximity. Low rheological contrasts between two magmas allow crystal transfer from a host magma into a basic magma (e.g., Barbarin and Didier 1992; Waight et al. 2000; Perugini et al. 2003). This transfer apparently occurred in the enclaves from the Harşit pluton (Fig. 2f), suggesting a mechanical transfer of the mineral grains during the mixing of the basic and felsic magmas while they behaved as liquids at depths. The similarities of the Sr–Nd–Pb isotopic compositions, in particular, are evidenced by the fact that the MMEs are not solid residues of a partial melting that represent a restitic origin. This observation, in fact, agrees well with both mixed and cognate origins. The inversely correlated I_{Sr} (79 Ma) ratios and ε_{Nd} (79 Ma) values in Fig. 8 clearly support the mixing process origin. The Harşit pluton does not display an adakitic signature, as is the case in the Saraycik pluton, the presence of which is consistent with an origin from the dehydration melting of the Pontide mafic lower crust (Topuz et al. 2005). Also, isotopic compositions of the Harşit pluton do not overlap with the fields of the Dölek and Sariçiçek plutons (~83% of enriched mantle contribution; Karsli et al. 2007) in the conventional isotope diagram (Fig. 8). To determine the possibility of mixing having taken place, we conducted isotopic modeling using a simple mixing model, the parameters of which are given above. Our calculations suggest that ~75% of lower crustal-derived melt and ~25% of enriched mantle-derived melt mixed at depth during the generation of the pluton (Fig. 12).

Underplating of a high-T, mantle-derived, basic magma and its interaction with the lower crust-derived magma has been recognized as the most favorable mechanism for the generation of hybrid magmas (e.g., Rudnick et al. 1986). This mechanism seems probable, as experimental studies show that underplating magma could provide the necessary

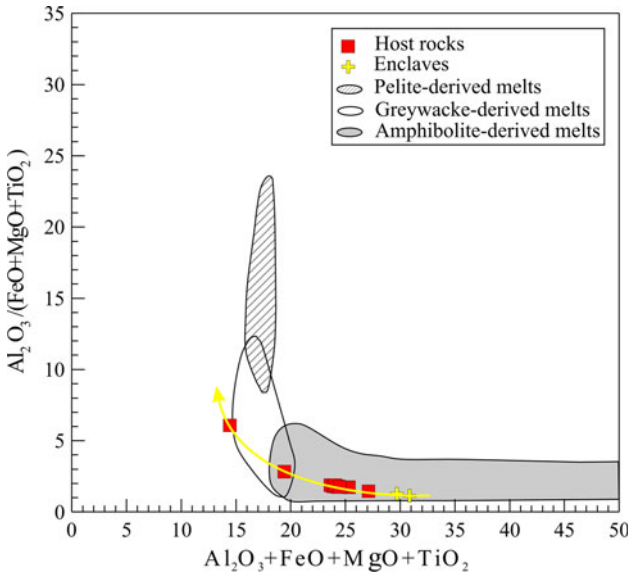

Fig. 11 Compositions of the Harşit rocks in comparison to compositional fields of experimentally derived partial melts of metapelites, metagreywackes and amphibolites. Data for experimentally derived liquids from Patiño Douce (1999)

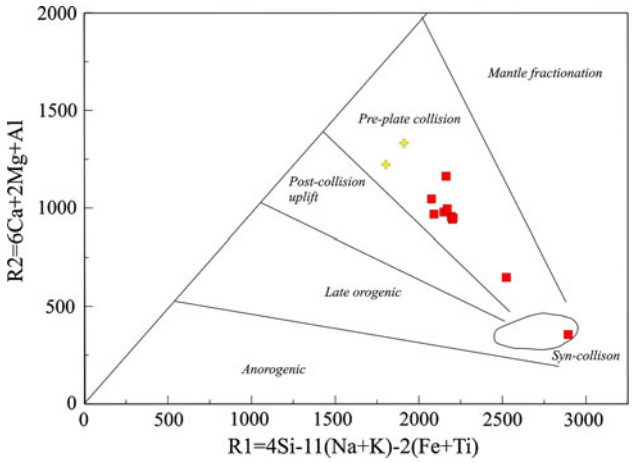

Fig. 12 R1–R2 diagram of Batchelor and Bowden (1985) for the Harşit samples. The Harşit samples fall into the pre-plate collision field. R1 = 4Si − 11(Na + K) − 2(Fe + Ti); R2 = 6Ca + 2 Mg + Al

heat source for the dehydration melting of lower crust (e.g., Rushmer 1991; Rapp and Watson 1995; Pedford and Gallagher 2001) and produce the granitic melt (e.g., Rushmer 1991; Tepper et al. 1993; Roberts and Clemens 1993; Wolf and Wyllie 1994; Rapp and Watson 1995). Topuz et al. (2005) and Karsli et al. (2007) also showed that the underplating mechanism could result in granitic melt by the dehydration melting of the lower crust in the Eastern Pontides.

Geodynamic scenario for the Harşit pluton

The heat sources for partial melting and the origin of middle Campanian, high-K calc-alkaline magmatism in the Eastern Pontides, Eastern Turkey have long been controversial issues. What is the cause of the melting of the lower crust and subcontinental lithospheric mantle beneath the Eastern Pontides in the late Mesozoic? The pluton studied was emplaced into the Cenomanian–Turonian subduction-related andesitic and dacitic volcanic lavas and their pyroclastics (Akin 1978; Okay and Şahintürk 1997; Okay and Tüysüz 1999). Hornblende separate from tonalite of the Harşit pluton yielded ages of 79 ± 4.3 Ma, which coincides with an ongoing northward subduction episode of the Izmir–Ankara–Erzincan oceanic slab (Şengör and Yilmaz 1981; Okay and Şahintürk 1997; Okay and Tüysüz 1999; Şengör et al. 2003; Altherr et al. 2008). The late Mesozoic magmatism in the eastern Pontides ranges from calc-alkaline to high-K calc-alkaline basalts and andesites formed in a rifted arc environment related to oceanic subduction (e.g., Okay and Şahintürk 1997; Yilmaz and Boztuğ 1996; Okay and Tüysüz 1999; Boztuğ et al. 2004, 2006; Altherr et al. 2008). Recently, a sporadic and small volume body of plagioleucitites (Maastrichtian to late Paleocene) with a high-potassic character in composition has been described by Altherr et al. (2008). In addition, subduction-related, high-K trachyandesites (ca. 80 Ma) genetically resembling the Harşit samples (Fig. 8) have been presented by Eyüboğlu (2010). The Senonian volcanic arc of the Eastern Pontides was an extensional arc, as illustrated by the submarine nature of the volcanism. In this case, the generation model and hybrid geochemistry with the mantle and lower crust-derived magmas suggest that this body was emplaced while the environment was under extensional conditions in a subduction zone rather than a post-collisional setting. There are two possibilities for tectonic scenarios in which high-K calc-alkaline magmas may be generated: (1) high-K, I-type rocks can occur in post-collisional setting similar to that of Caledonia (Pitcher 1987), where melting of the source rocks is caused by decompression following crustal thickening. (2) high-K rocks are emplaced and erupted in a continental arc setting similar to that of the Andes (Pitcher 1987). The chemistry and isotopic compositions of the calc-alkaline granitoid magmas in these tectonic environments are thought to reflect a mixture of enriched subcontinental lithospheric mantle-derived and lower crustal-derived magmas. In the region a subduction environment is proposed at a time of 79 Ma based on the presence of an accretionary complex described by Okay and Tüysüz (1999) resting on the lower Cretaceous pelagic carbonates and uncomformably overlain by Maastrichtian limestones (Ketin 1951; Fenerci 1994; Okay and Tüysüz 1999). In addition, major crustal shortening in the eastern Pontides occurred during the

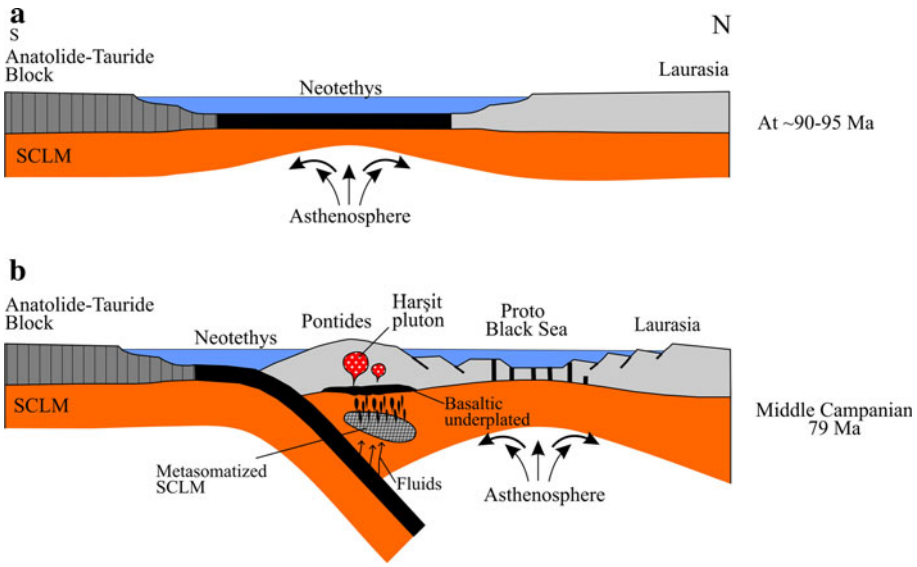

Fig. 13 Schematic illustration for the late Mesozoic geodynamic evolution of the Eastern Pontides. **a** At ~90–95 Ma, the İzmir–Ankara–Erzincan oceanic slab reached its maximum enlargement (e.g., Akin 1979; Şengör and Yilmaz 1981; Okay and Şahintürk 1997; Okay and Tüysüz 1999). **b** At somewhere before 79 Ma, passive margin of the Eastern Pontides transformed into an Andean type margin. Then, the slab subducted beneath the Eurasian block (Okay and Şahintürk 1997; Okay et al. 1997; Altherr et al. 2008). The duration of subduction extends from Turonian to late Maastrichtian and Danian, which places tight constraints in the region (e.g., Okay and Tüysüz 1999). During the middle Campanian period (79 Ma) in the Eastern Pontides, with beginning of opening of the East Black Sea Basin, the Eastern Pontide was an extensional arc as suggested by the submarine nature of the volcanism. The extensional phase cause melting of the enriched SCLM. The mafic underplated results in extensive melting of lower crustal rocks of the Eastern Pontide block. Then, the two melts mixed and underwent fractional crystallization to form the Harşit granitoid rocks from the Eastern Pontides

Paleocene and early Eocene (e.g., Okay and Tüysüz 1999). Then, Karsli et al. (2010) claimed that the first stage of post-collision extensional events following crustal thickening started at ~50 Ma. Accordingly, the R1–R2 classification diagram of the pluton, developed by Batchelor and Bowden (1985) to explain the specific tectonic setting, suggests a pre-plate collision phase for the Harşit rocks. Also, a Maastrichtian–Paleocene plagioleucitite body in the Bayburt area from the eastern Pontides is thought to be last products of northward subduction of the northern branch of Neotethys (Altherr et al. 2008). Therefore, these considerations weaken the possibility of generation of high-K calc-alkaline magmas in a post-collision extensional setting in the region. Hence, the generation of high-K calc-alkaline granitic magmas in a subduction zone at ~79 Ma in the eastern Pontides appears likely. In modeling of upper Cretaceous northward subduction (Şengör and Yilmaz 1981; Okay and Tüysüz 1999; Şengör et al. 2003; Altherr et al. 2008), since the southern margin of the Neotethys Ocean was passive, subducted crust would progressively become cold and older (Fig. 13a). The over-riding continental plate rapidly thins by extension developed in a back-arc basin (namely, the Black Sea). The marginal basins behind extensional arcs usually develop by the splitting of the volcanic arc axis (e.g., Karig 1971). Hence, the East Black Sea basin probably started to open during the middle Campanian (~79 Ma) by the splitting of this arc axis. Calc-alkaline magmas can be formed by decompression melting of continental lithosphere previously modified by subduction (Hawkesworth et al. 1993; Wilson et al. 1997; Fan et al. 2003). Fluids from the dehydration of the slab cause enrichment of the lithospheric mantle. Hence, the enriched mantle can induce mafic melts, which intrude into the base of the lower crust. In this way, underplated basaltic magma, together with the considerable amount of heat required for melting above the plagioclase stability field at lower crustal depths, could have been provided (Fig. 13b). Additionally, underplating of mantle magma can induce the melting of the lower crust, and the two magmas can then mix at the depth of the lower crustal levels. Underplating is a well-known mechanism for the genesis of hybrid granitoid rocks and is also adopted herein. The timing of the underplating is believed to be closely related to major episodes of regional tectonics and also to the geodynamic processes in the deep parts of the subcontinental lithosphere. The ^{40}Ar–^{39}Ar amphibole age of 79 Ma of the Harşit pluton refers to the middle Campanian pre-plate collisional stage during its generation. The high-K nature, small Eu anomalies, the compositional range from gabbroic diorite to granite and negative ε_{Nd} (t) values can all be explained by the presence of a mafic lower crust and a chemically enriched mantle as end-members in a subduction zone, where the back-arc extensional events started at least by ~79 Ma in the Eastern Pontides.

Conclusions

Based on the integrated Sr–Nd–Pb, geochemical and geochronological analyses of the host rocks and their MMEs, the following scenario for the Harşit pluton from the Eastern Pontides could be given; the emplacement of the pluton, which is I-type and mostly metaluminous characteristics and belongs to the high-K calc-alkaline series, took place at ~79 Ma (middle Campanian) as revealed by the Ar–Ar ages on the hornblende separate.

The Sr–Nd mixing modeling allowed more precise identification and even rough quantification of the two main source components (lower crust, 65–75% and lithospheric mantle, 25–35%), which are responsible for the magma genesis of the pluton. The mixing of two end-members was followed by the fractional crystallization of plagioclase, amphibole, biotite and Fe–Ti oxides during the rock generation. Also, the Sr–Nd and geochemical data reveal that the upper crustal assimilation appears plausible in generation of the pluton.

The geochemical and isotopic compositions and tectonomagmatic properties suggest the Harşit rocks formed in a subduction zone. The beginning of subducting of Neotethys oceanic crust beneath the eastern Pontides in Cenomanian–Turonian could account for the arc-related volcanism. With ongoing subduction, the slab-derived fluids added to mantle component cause partial melting of the subcontinental lithospheric mantle, which induced underplated mafic melt. The underplated mafic melt results in partial fusion of the lower part of the Pontide lower crust. Then two magma mixed in the some proportion, as suggested above, to generate hybrid Harşit magma in an extensional arc environment at ~79 Ma in the eastern Pontides. Hence, the back-arc extensional events, resulting in the opening of East Black Sea Basin, could be formed at least middle Campanian (~79 Ma) in the Eastern Pontides.

Acknowledgments This work was supported by the Scientific and Technological Research Council of Turkey (TÜBITAK) with grants # 107Y177 and 108Y200. The authors are also grateful to Durmuş Boztuğ and Hakan Çoban for their critical and constructive comments. Ahmet D. Şen and Murat Ketenci are thanked for their enthusiastic assistances during fieldwork.

References

Aguillón-Robles A, Caimus T, Bellon H, Maury RC, Cotton J, Bourgois J, Michaud F (2001) Late Miocene adakites and Nb-enriched basalts from Vizcaino Peninsula, Mexico: indicators of East Pacific Rise subduction below southern Baja California. Geology 29:531–534

Akin H (1979) Geologie, magmatismus und Lagerstattenbildung im ostpontischen Gebirge/Türkei aus der Sicht der Plattentektonik. Geol Rundschau 68:253–283

Altherr R, Henjes-Kunst F, Langer C, Otto J (2000) Interaction between crustal-derived felsic and mantle-derived mafic magmas in the Oberkirch Pluton (Eoropean Variscides, Schwarzwald, Germany). Contrib Mineral Petrol 137:304–322

Altherr R, Topuz G, Siebel W, Şen C, Meyer H-P, Satır M (2008) Geochemical and Sr–Nd–Pb isotopic characteristics of Paleocene plagioleucitites from the Eastern Pontides (NE Turkey). Lithos 105:149–161

Avagyan A, Sosson M, Philip MH, Karakhanian A, Rolland Y, Melkonyan R, Rebai S, Davtyan V (2005) Neogene to Quaternary stress field evolution in Lesser Caucasus and adjacent regions using fault kinematics analysis and volcanic cluster data. Geodin Acta 18:401–416

Barbarin B (1999) A review of the relationships between granitoid types, their origins and their geodynamic environments. Lithos 46:605–626

Barbarin B, Didier J (1992) Genesis and evolution of mafic microgranular enclaves through various types of interaction between coexisting felsic and mafic magmas. Trans R Soc Earth Sci 83:145–153

Batchelor RA, Bowden P (1985) Petrogenetic interpretation of granitoid rock series using multicationic parameters. Chem Geol 48:43–55

Bonin B (2004) Do coeval mafic and felsic magmas in post-collisional to within-plate regimes necessarily imply two contrasting, mantle and crustal, sources? A review. Lithos 78:1–24

Boynton WV (1984) Cosmochemistry of the rare earth elements: meteorite studies. In: Henderson P (ed) Rare earth element geochemistry. Elsevier, Amsterdam, pp 63–114

Boztuğ D, Jonckheere R, Wagner GA, Yeğingil Z (2004) Slow Senonian and fast Paleocene–Early Eocene uplift of the granitoids in the Central Eastern Pontides, Turkey: apatite fission-track results. Tectonophysics 382:213–228

Boztuğ D, Erçin AI, Kuruçelik MK, Göç D, Kömür I, Iskenderoğlu A (2006) Geochemical characteristics of the composite Kackar batholith generated in a Neo-Tethyan convergence system, eastern Pontides, Turkey. J Asian Earth Sci 27:286–302

Cameron BI, Walker JA, Carr MJ, Patino LC, Matias O, Feigenson MD (2003) Flux versus decompression melting at stratovolcanos in southeastern Guatemala. J Volcanol Geotherm Res 119:21–50

Castillo PR, Janney PE, Solidum RU (1999) Petrology and geochemistry of Camiguin island, southern Philippines: insights to the source of adakites and other lavas in a complex arc setting. Contrib Mineral Petrol 134:33–51

Chappell BW (1999) Aluminum saturation in I- and S-type granites and the characterization of fractionated hapogranites. Lithos 46:531–551

Chappell BW, White AJR (1992) I- and S-type granites in the Lachlan Fold Belt. Trans R Soc Edinb Earth Sci 83:1–26

Chen B, Arakawa Y (2005) Elemental and Nd–Sr isotopic geochemistry of granitoids from the West Jungar foldbelt (NW China), with implications for phanerozoic continental growth. Geochim Cosmochim Acta 69:1307–1320

Chen B, Jahn BM (2004) Genesis of post-collisional granitoids and basement nature of the Junggar Terrane, NW China: Nd–Sr isotope and trace element evidence. J Asian Earth Sci 23:691–703

Chen B, Jahn BM, Wei C (2002) Petrogenesis of Mesozoic granitoids in the Dabie UHP complex, Central China: trace element and Nd–Sr isotope evidence. Lithos 60:67–88

Chen B, Jahn BM, Zhai MG (2003) Sr–Nd isotopic characteristics of the Mesozoic magmatism in the Taihang–Yanshan orogen, north China craton, and implications for Archean lithosphere thinning. J Geol Soc Lond 160:963–970

Defant MJ, Jackson TE, Drummond MS, De Boer JZ, Bellon H, Feigenson MD, Maury RC, Stewart RH (1992) The

geochemistry of young volcanism throughout western Panama and southeastern Costa Rica: an overview. J Geol Soc Lond 149:569–579

Dokuz A (2009) Hercynian pre-syn-collisional granitic rocks from the Gümüşhane are, Northeastern Turkey: implications for magma mixing and tectonic setting. Lithos (in review)

Dokuz A, Tanyolu E, Genç S (2006) A mantle- and a lower crust-derived bimodal suite in the Yusufeli (Artvin) area, NE Turkey: trace element and REE evidence for subduction-related rift origin of Early Jurassic Demirkent intrusive complex. Int Earth Sci 95:370–394

Dokuz A, Karsli O, Chen B, Uysal I (2010) Sources and petrogenesis of Jurassic granitoids in the Yusufeli area, Northeastern Turkey: implication for pre- and post-collisional lithospheric thinning of the Eastern Pontides. Tectonophysics 480:259–279

Eyüboğlu Y (2010) Late Cretaceous high-K volcanism in the Eastern Pontide orogenic belt: implications for the geodynamic evolutions of NE Turkey. Int Geol Rev 52:142–186

Fan W-M, Guo F, Wang Y-J, Lin G (2003) Late Mesozoic calc-alkaline volcanism of post orogenic extension in the Northern Da Hinggan Mountains, northeastern China. J Volcanol Geotherm Res 121:115–135

Fenerci M (1994) Rudists from Maden (Bayburt) area (NE Turkey). Turk J Earth Sci 3:1–12

Ferré EC, Bernard EL (2001) Geodynamic significance of early orogenic high-K crustal and mantle melts: example of the Corsica Batholith. Lithos 59:47–67

Flierdt T, Hoernes S, Jung S, Masberg P, Hoffer E, Schaltegger U, Friedrichsen H (2003) Lower crustal melting of syn-orogenic quartz diorite–granite–leucogranite associations: constraints from Sr–Nd–O isotopes from the Bandombaai Complex, Namibia. Lithos 67:205–226

Frost BR, Mahood GA (1987) Field, chemical and physical constraints on mafic–felsic interaction in the Lamarck granodiorite, Sierra Nevada, California. Geol Soc Am Bull 99:272–291

Frost CD, Frost BR, Chamberlain KR, Hulsebosch TP (1998) The Late Archean history of the Wyoming province as recorded by granitic magmatism in the Wind River Range, Wyoming. Precamb Res 89:145–173

Grove TL, Donnelly-Nolan JM (1986) The evolution of young silicic lavas at Medicine lake Volcano, California: implications for the origin of compositional gaps in calc-alkaline series lavas. Contrib Mineral Petrol 92:281–302

Han BF, Wang SG, Jahn BM, Hong DW, Kagami H, Sun YL (1997) Depleted mantle source for the Ulungur River A-type granites from North Xinjiang, China: geochemistry and Nd–Sr isotopic evidence and implications for Phanerozoic crustal growth. Chem Geol 138:135–159

Harland WB, Armstrong RL, Cox AV, Craig LE, Smith AG, Smith DG (1990) A geologic time scale 1989. Cambridge University Press, revised edn, p 279

Hart S (1984) A large scale isotopic anomaly in the southern hemisphere mantle. Nature 47:753–757

Hawkesworth CJ, Gallagher K, Herot JM, McDermott F (1993) Mantle and slab contributions in arc magmas. Ann Rev Earth Planet Sci 21:175–2004

Hibbard MJ (1991) Textural anatomy of twelve magma-mixed granitoid systems. In: Didier J, Barbarin B (eds) Enclaves and granite petrology. Dev Petrol 13. Elsevier, Amsterdam, pp 431–444

Karig DE (1971) Origin and development of the marginal basins in the Western Pacific. J Geophys Res 76:2542–2561

Karsli O, Aydin F, Sadiklar MB (2002) Geothermobarometric investigation of the Zigana Granitoid, eastern Pontides, Turkey. Int Geol Rev 44:277–286

Karsli O, Aydin F, Sadiklar MB (2004a) Magma interaction recorded in plagioclase zoning in granitoid systems, Zigana Granitoid, Eastern Pontides, Turkey. Turk J Earth Sci 13:287–305

Karsli O, Aydin F, Sadiklar MB (2004b) The morphology and chemistry of K-feldspar megacrysts from İkizdere Pluton: evidence for acid and basic magma interactions in granitoid rocks, NE Turkey. Chem Erde-Geochem 64:155–170

Karsli O, Chen B, Aydin F, Şen C (2007) Geochemical and Sr–Nd–Pb isotopic compositions of the Eocene Dölek and Sariçiçek Plutons, Eastern Turkey: implications for magma interaction in the genesis of high-K calc-alkaline granitoids in a post-collision extensional setting. Lithos 98:67–96

Karsli O, Chen B, Uysal I, Aydin F, Wijbrans RJ, Kandemir R (2008) Elemental and Sr–Nd–Pb isotopic geochemistry of the most recent Quaternary volcanism in the Erzincan Basin, Eastern Turkey: framework for the evaluation of basalt-lower crust interaction. Lithos 106:55–70

Karsli O, Dokuz A, Uysal I, Aydin F, Kandemir R, Wijbrans RJ (2010) Generation of the Early Cenozoic adakitic volcanism by partial melting of mafic lower crust, Eastern Turkey: implications for crustal thickening to delamination. Lithos 114:109–120

Kay SM, Ramos VA, Marquez M (1993) Evidence in Cerro Pampa volcanic rocks of slab melting prior to ridge trench collision in southern South America. J Geol 101:703–714

Kaygusuz A, Siebel W, Şen C, Satir M (2008) Petrochemistry and petrology of I-type granitoids in an arc setting: the composite Torul pluton, Eastern Pontides, NE Turkey. Int J Earth Sci 97:739–764

Kempton PD, Downes H, Embey-Istzin A (1997) Mafic granulite xenoliths in Neogene alkali basalts from the Western Pannonian Basin: insights into the lower crust of a collapsed orogen. J Petrol 38:941–970

Ketin I (1951) Bayburt bölgesinin jeolojisi hakkinda. Istanbul Universitesi Fen Fakultesi Mecmuasi 21:113–127

Koçyiğit A, Yilmaz A, Adamia S, Kuloshvili S (2001) Neotectonics of East Anatolian Plateau (Turkey) and Lesser Caucasus: implication for transition from thrusting to strike–slip faulting. Geodin Acta 14:177–195

Kumar S, Rino V, Pal AB (2004) Field evidence of magma mixing from microgranular enclaves hosted in Palaeoproterozoic Malanjkhand granitoids, Central India. Gondwana Res 7:539–548

Liu HT, Sun SH, Liu JM, Zhai MG (2002) The Mesozoic high-Sr granitoids in the northern marginal region of North China craton: geochemistry and source region. Acta Petrol Sin 18:257–274

Lopéz S, Castro A (2001) Determination of the fluid-absent solidus and supersolidus phase relationships of MORB-derived amphibolites in the range 4–14 kbar. Am Mineral 86:1396–1403

Mahoney JJ, Frei R, Tejada MLG, Mo XX, Leat PT, Nagler TP (1998) Tracing the Indian Ocean mantle domain through time: isotopic results from old west Indian, east Tethyan and South Pacific seafloor. J Petrol 39:1285–1306

Maniar PD, Piccoli PM (1989) Tectonic discrimination of granitoids. Bull Am Geol Soc 101:635–643

Mason PRD, Downes H, Thirlwall MF, Seghedi I, Szakács A, Lowry D, Mattery D (1996) Crystal assimilation as a major petrogenetic process in the East Carpathian Neogene and Quaternary continental margin arc, Romania. J Petrol 37:927–959

Middlemost EAK (1994) Naming materials in the magma/igneous rock system. Earth Sci Rev 37:215–224

Moore WJ, McKee EH, Akinci Ö (1980) Chemistry and chronology of plutonic rocks in the Pontide Mountains, Northern Turkey. Symposium of European Copper Deposit, Belgrade, pp 209–216

Okay AI, Şahintürk Ö (1997) Geology of the Eastern Pontides. In: Robinson AG (ed) Regional and petroleum geology of the Black Sea and surrounding region. AAPG Memoir 68:292–311

Okay AI, Tüysüz O (1999) Tethyan sutures of northern Turkey. In: Durand B, Jolivet L, Horvath F, Seranne M (eds) The Mediterranean Basins: tertiary extension within the Alpine orogen. Geol Soc Spec Publ 156:475–515

Okay AI, Şahintürk Ö, Yakar H (1997) Stratigraphy and tectonics of the Pulur (Bayburt) region in the eastern Pontides. Mineral Res Exp Bull 119:1–24

Patiño Douce AE (1999) What do experiments tell us about the relative contributions of crust and mantle to the origin of granitic magmas? In: Castro A, Fernandez C, Vigneresse JL (eds) Understanding granites: integrating new and classical techniques. Geol Soc Lond 168:55–75

Peccerillo A, Taylor SR (1976) Geochemistry of Eocene calc-alkaline volcanic rocks from Kastamonu area, northern Turkey. Contrib Mineral Petrol 58:63–81

Pedford N, Gallagher K (2001) Partial melting of mafic (amphibolitic) lower crust by periodic influx of basaltic magma. Earth Planet Sci Lett 193:483–499

Perugini D, Poli G (2000) Chaotic dynamics and fractals in magmatic interaction processes: a different approach to the interpretation of mafic microgranular enclaves. Earth Planet Sci Lett 175:93–103

Perugini D, Poli G, Christofides G, Eleftheriadis G (2003) Magma mixing in the Sithonia Plutonic Complex, Greece: evidence from mafic microgranular enclaves. Mineral Petrol 78:173–200

Pitcher WS (1987) Granites and yet more granites forty years on. Geol Rundschau 76:51–79

Poli GE, Tommasini S (1991) Model for the origin and significance of microgranular enclaves in calc-alkaline granitoids. J Petrol 32:657–666

Qiao G (1988) Normalization of isotopic dilution analyses—a new program for isotope mass spectrometric analysis. Sci Sin 31:1263–1268

Rapp RP, Watson EB (1995) Dehydration melting of metabasalt at 8–32 kbar: implications for continental growth and crust–mantle recyling. J Petrol 36:891–931

Rapp RP, Watson EB, Miller CF (1991) Partial melting of amphibolite/eclogite and the origin of Archean trondhjemites and tonalities. Precamb Res 51:1–25

Roberts MP, Clemens JD (1993) Origin of high-potassium, calc-alkaline, I-type granitoids. Geology 21:825–828

Robinson AG, Banks CJ, Rutherford MM, Hirst JPP (1995) Stratigraphic and structural development of the Eastern Pontides, Turkey. J Geol Soc Lond 152:861–872

Rottura A, Bargossi GM, Caggianelli A, Del Moro A, Visona D, Tranne CA (1998) Origin and significance of the Permian high-K calc-alkaline magmatism in the central-eastern Southern Alps, Italy. Lithos 45:329–348

Rudnick RL, McDonough WF, McCulloch MT, Taylor SR (1986) Lower crustal xenoliths from Queensland, Australia: evidence for deep crustal assimilation and fractionation of continental basalts. Geochim Cosmochim Acta 50:1099–1115

Rushmer T (1991) Partial melting of two amphibolites: contrasting experimental results under fluid-absent conditions. Contrib Mineral Petrol 107:41–59

Sajona FG, Naury RC, Pubellier M, Leterrier J, Bellon H, Cotton J (2000) Magmatic source enrichment by slab-derived melts in a young post-collision setting, central Mindanao (Philippines). Lithos 54:173–206

Şen C, Dunn T (1994) Dehydration melting of a basaltic composition amphibolite at 1.5 and 2.0 GPa: implications for the origin of adakites. Contrib Mineral Petrol 117:394–409

Şen C, Arslan M, Van A (1998) Geochemical and petrological characteristics of the Eastern Pontide Eocene (?) alkaline volcanic province, NE Turkey. Turk J Earth Sci 7:231–239

Şengör AMC, Yilmaz Y (1981) Tethyan evolution of Turkey: a plate tectonic approach. Tectonophysics 75:181–241

Şengör AMC, Özeren S, Genç T, Zor E (2003) East Anatolian high plateau as a mantle-supported, North–south shortened domal structure. Geophys Res Lett 30(24):8045. doi:10.1029/2003GL017858

Soesoo A (2000) Fractional crystallization of mantle-derived melts as a mechanism for some I-type granite petrogenesis: an example from Lachlan Fold Belt, Australia. J Geol Soc 157:135–149

Sonder LJ, England PC, Wernicke BP, Christiansen RL (1987) A physical model for Cenozoic extension of western North America. Geol Soc Spec Publ 28:187–201

Springer W, Seck HA (1997) Partial fusion of basic granulites at 5 to 15 kbar: implications for the origin of TTG magmas. Contrib Mineral Petrol 127:30–45

Sun SS, McDonough WE (1989) Chemical and isotopic systematics of oceanic basalts: implications for mantle composition an processes. In: Saunders AD, Norry MJ (eds) Magmatism in the ocean basins. Geol Soc Spec Publ, pp 313–345

Taner MF (1977) Etuda geologique et petrographique de la region de Güneyce-İkizdere, situee au sud de Rize (Pontides orientalas, Turquie). PhD Thesis, Universite de Geneve, 180 p (unpublished)

Tepper JH, Nelson BK, Bergantz GW, Irving AJ (1993) Petrology of the Chilliwack batholith, North Cascades, Washington: generation of calc-alkaline granitoids by melting of mafic lower crust with variable fugacity. Contrib Mineral Petrol 113:333–351

Thirlwall MF, Jones NW (1993) Isotope geochemistry and contamination mechanism of Tertiary lavas from Skye, northwest Scotland. In: Hawkesworth CJ, Norry MJ (eds) Continental basalts and mantle xenoliths. Shiva, Cheshire, pp 186–208

Tokel S (1977) Doğu Karadeniz Bölgesinde Eosen yaşlı kalk-alkalen andezitler ve jeotektonizma. Türkiye Jeoloji Bülteni 20:49–54

Topuz G, Altherr R, Schwarz WH, Siebel W, Satir M, Dokuz A (2005) Post-collisional plutonism with adakite-like signatures: the Eocene Saraycik granodiorite (Eastern Pontides, Turkey). Contrib Mineral Petrol 150:441–455

Tribuzio R, Thirlwall MF, Vannucci R, Matthew F (2004) Origin of the gabbro–peridotite association from the Northern Apennine Ophiolites (Italy). J Petrol 45:1109–1124

Turner SP, Foden JD, Morrison RS (1992) Derivation of some A-type magmas by fractionation of basaltic magma: an example from the Padthaway Ridge, South Australia. Lithos 28:151–179

Varol E, Temel A, Gourgaud A, Bellon H (2007) Early Miocene 'adakite-like' volcanism in the Balkuyumcu region, central Anatolia, Turkey: petrology and geochemistry. J Asian Earth Sci 30:613–628

Vernon RH (1984) Microgranitoid enclaves in granites-globules of hybrid magma quenched in a plotonic environment. Nature 309:438–439

Vernon RH (1990) Crystallization and hybridism in microgranitoid enclave magmas: microstructural evidence. J Geophys Res 95:17849–17859

Volkert RA, Feigenson MD, Patino LC, Delaney JS, Drake AA Jr (2000) Sr and Nd isotopic compositions, age and petrogenesis of A-type granitoids of the Vernon Supersuite, New Jersey Highlands, USA. Lithos 50:325–347

Waight TE, Maas R, Nicholls IA (2000) Fingerprinting feldspar phenocrysts using crystal isotopic composition stratigraphy: implications for crystal and magma mingling in S-type granites. Contrib Mineral Petrol 139:227–239

Wiebe RA (1991) Commingling of contrasted magmas and generation of mafik enclaves in granitic rocks. In: Didier J, Barbarin B (eds) Enclaves and granite petrology. Dev Petrol 13:393–402

Wiebe RA (1996) Mafic–silicic layered intrusions: the role of basaltic injections on magmatic processes and evolution of silicic magma chambers. Trans R Soc Edinb Earth Sci 87:233–242

Wijbrans JR, Pringle MS, Koppers AAP, Scheveers R (1995) Argon geochronology of small samples using the Vulcaan argon laser probe. Processes Kon Ned Akad V Wetensh 98:185–218

Wilson M, Tankut A, Guleç N (1997) Tertiary volcanism of the Galatia province, north-west Central Anatolia, Turkey. Lithos 42:105–121

Windley BF (1991) Early Proterozoic collision tectonics, and rapakivi granites as intrusions in an extensional thrust-thickened crust: the Ketilidian orogen. Tectonophysics 195:1–10

Winther KT (1996) An experimentally based model for the origin of tonalitic and throndhjemitic melts. Chem Geol 127:43–59

Wolf MB, Wyllie PJ (1994) Dehydration-melting of amphibolite at 10 kbar: the effects of temperature and time. Contrib Mineral Petrol 115:369–383

Wyllie PJ, Wolf MB (1993) Amphibolite dehydration-melting: sorting out the solidus. In: Prichard HM, Alabaster T, Harris NBW, Neary CR (eds) Magmatic processes and plate tectonics. Geol Soc Spec Publ 76:405–416

Xu JF, Castillo PR (2004) Geochemical and Nd–Pb isotopic characteristics of the Tethyan asthenosphere: implications for the origin of the Indian Ocean mantle domain. Tectonophysics 393:9–27

Xu JF, Castillo PR, Chen FR, Niu HC, Yu XY, Zhen ZP (2003) Geochemistry of late Paleozoic mafic igneous rocks from the Kuerti area, Xinjiang, northwest China: implications for backarc mantle evolution. Chem Geol 193:137–154

Yang JH, Fu Y, Wu FY, Wilde SA, Xie LW, Yang YH, Liu XM (2007) Tracing magma mixing in granite genesis: in situ U–Pb dating and Hf-isotope analysis of zircons. Contrib Mineral Petrol 153:177–190

Yilmaz Y (1972) Petrology and structure of the Gümüşhane granite and the surrounding rocks. NE Anatolia, PhD thesis, University College London, pp 248

Yilmaz S, Boztuğ D (1996) Space and time relations of three plutonic phases in the Eastern Pontides, Turkey. Int Geol Rev 38:935–956

Yilmaz Y, Tüysüz O, Yiğitbaş E, Genç ŞC, Şengör AMC (1997) Geology and tectonic evolution of the Pontides. In: Robinson AG (ed) Regional and petroleum geology of the Black Sea and surrounding region. Am Assoc Petrol Geol Mem 68:183–226

Zindler A, Hart SR (1986) Chemical geodynamics. Ann Rev Earth Planet Sci 14:493–571